



# Integrated Space-Time Dataset Reveals High Diversity and Distinct Community Structure of Ciliates in Mesopelagic Waters of the Northern South China Sea

Ping Sun<sup>1,2\*</sup>, Liying Huang<sup>1</sup>, Dapeng Xu<sup>3</sup>, Alan Warren<sup>4</sup>, Bangqin Huang<sup>2</sup>, Ying Wang<sup>1</sup>, Lei Wang<sup>1</sup>, Wupeng Xiao<sup>1</sup> and Jie Kong<sup>1</sup>

<sup>1</sup> Key Laboratory of the Ministry of Education for Coastal and Wetland Ecosystem, College of the Environment and Ecology, Xiamen University, Xiamen, China, <sup>2</sup> Fujian Provincial Key Laboratory for Coastal Ecology and Environmental Studies, Xiamen University, Xiamen, China, <sup>3</sup> State Key Laboratory of Marine Environmental Science, Institute of Marine Microbes and Ecospheres, College of Ocean and Earth Sciences, Xiamen University, Xiamen, China, <sup>4</sup> Department of Life Sciences, Natural History Museum, London, United Kingdom

## OPEN ACCESS

### Edited by:

Jackie L. Collier,  
Stony Brook University, United States

### Reviewed by:

Feng Zhao,  
Institute of Oceanology (CAS), China  
Luciana Santoferrara,  
University of Connecticut,  
United States

### \*Correspondence:

Ping Sun  
psun@xmu.edu.cn

### Specialty section:

This article was submitted to  
Aquatic Microbiology,  
a section of the journal  
Frontiers in Microbiology

**Received:** 17 June 2019

**Accepted:** 05 September 2019

**Published:** 24 September 2019

### Citation:

Sun P, Huang L, Xu D, Warren A, Huang B, Wang Y, Wang L, Xiao W and Kong J (2019) Integrated Space-Time Dataset Reveals High Diversity and Distinct Community Structure of Ciliates in Mesopelagic Waters of the Northern South China Sea. *Front. Microbiol.* 10:2178. doi: 10.3389/fmicb.2019.02178

Little is known about diversity distribution and community structure of ciliates in mesopelagic waters, especially how they are related to spatial and temporal changes. Here, an integrative approach, combining high-throughput cDNA sequencing and quantitative protargol stain, was used to analyze ciliate communities collected temporally along a transect from coastal to oceanic regions at depths ranging from the surface to 1000 m. The mesopelagic zone exhibited comparable alpha diversity to surface water which was consistent over temporal variation, with high diversity occurring at the interface with the euphotic zone. Comparison with the northeastern and the western Pacific Ocean revealed consistency of this vertical distribution of ciliates across oceanic basins. Mesopelagic ciliates harbored distinct community structure without significant seasonal differences, with the vertical variations driven largely by members of the classes Spirotrichea and Oligohymenophorea. Operational taxonomic units (OTUs) affiliated with Scuticociliatia, Astomatida and Apostomatida, members of which are known to be bacterivorous and/or commensal/parasitic species, were more abundant in mesopelagic waters than above, implying they are an important component of food webs in the mesopelagic zone. A combination of depth, geographic distance and environment shaped the ciliate communities, with depth being the most influential factor. Phylogenetic null modeling analysis further indicated that 57.1 and 33.3% of mesopelagic community variation was governed by dispersal limitation and heterogeneous selection, respectively, probably due to the marked biochemical and physical gradients down the water column. This suggests that ciliate community structure in the mesopelagic zone is mainly controlled by stochastic processes. Collectively, this study reports mesopelagic ciliates exhibited high

diversity and distinct community structure across spatiotemporal scales and informs the processes mediating ciliate assembly in the mesopelagic zone. These should be fully considered in future studies to build a more comprehensive understanding of mesopelagic microbial assemblages.

**Keywords:** ciliates, diversity, community structure, assembly mechanism, high throughput cDNA sequencing, quantitative protargol stain, mesopelagic zone

## INTRODUCTION

The mesopelagic realm is a vast, dimly lit region that spans the globe between about 200–1,000 m beneath the ocean's surface. It is also the zone where 90% of the organic carbon exported from epipelagic waters is remineralized (Robinson et al., 2010). By their grazing on particulate organic matter such as bacteria and other microorganisms, ciliates act as active regulators of biogeochemical processes and nutrient cycling and thus play key roles in mesopelagic ecosystem function (Tanaka and Rassoulzadegan, 2002; Gowing et al., 2003). Therefore, knowledge of ciliate diversity distribution, community structure and assembly mechanisms are needed in order to improve understanding of the microbial ecology in the mesopelagic zone.

Despite limited studies, contrasting findings have been reported in terms of ciliate diversity distribution (Wickham et al., 2011; Grattepanche et al., 2016). For example, both microscopy- and 18S rRNA gene clone library-based studies showed that ciliate abundance and species richness decrease with the increasing water depth, the low abundance of prokaryotes as a food resource in the waters below the euphotic zone being cited as the most likely cause (Tanaka and Rassoulzadegan, 2002; Countway et al., 2010; Wickham et al., 2011). By contrast, a study of two major lineages of planktonic ciliates off the coast of New England employing high-throughput sequencing (HTS) of the hyper variable V2 region of the rRNA gene revealed that alpha-diversity increased with increasing depth, the highest diversity occurring below the photic zone (50–800 m) (Grattepanche et al., 2016). In order to resolve this discrepancy, studies that employ a combination of both morphology- and molecular-based methods to analyze ciliate diversity down the water column over spatial and temporal scales are required.

Compared with the photic zone, studies of mesopelagic ciliates are limited and mainly focus on their abundance and biomass (Gowing et al., 2003; Hu et al., 2016; Zhao et al., 2017; Dolan et al., 2019). Addressing the assembly mechanisms impacting microbial communities, which is important to strengthen our understanding of the ecological processes mediating community assembly of microorganisms, has recently received more attention (Stegen et al., 2013; Zhou and Ning, 2017; Logares et al., 2018). The relative importance of deterministic vs. stochastic processes depends on spatial and temporal scales, species traits and the local environment (Dolan et al., 2007; Doherty et al., 2010) which, to the best of our knowledge, have never been evaluated for mesopelagic ciliates.

The South China Sea (SCS) is one of the largest marginal seas in the western Pacific Ocean, with an area of about 3.3 million km<sup>2</sup> and a depth ranging from the shallowest coastal

fringe to a maximum of more than 5000 m (Liang et al., 2008). The northeastern SCS is connected to the western Pacific Ocean by the Luzon Strait, which has a sill depth of about 1900 m. The SCS is located within the range of the monsoon regime and is affected by the southwest monsoon in summer and the northeast monsoon in winter (Morton and Blackmore, 2001).

In this study, a combination of morphology-based quantitative protargol stain (QPS) and 18S rRNA gene transcript-based HTS approaches were employed to investigate the diversity and community structure of ciliates along a coast-to-oceanic transect in the northern region of the SSC. Samples were collected at various depths from the surface to the mesopelagic zone (1000 m deep) in spring and summer of the years 2013 and 2014, respectively. Employing morphological or molecular approaches, previous studies have revealed a distinct vertical distribution of alpha diversity, i.e., diversity increases/decreases with depth (Countway et al., 2010; Wickham et al., 2011; Grattepanche et al., 2016). The first question explored here is whether or not the diversity of ciliates down the water column, revealed by a combination of morphological and molecular approaches, is consistent with either of the previous findings. Mesopelagic ciliates occupy distinct ecological niches and play differential ecological functions compared to members of the photic zone (Gowing et al., 2003; Zhao et al., 2017). Therefore, the second question explored here is the membership of the mesopelagic ciliate assemblage differs from that of overlying communities. Thirdly, we investigate whether mesopelagic ciliates show temporal patterns of distribution and the ecological processes that shape ciliate assembly in mesopelagic zone.

## MATERIALS AND METHODS

### Sampling and Environmental Factors Analyses

Samples were collected from five sites separated by 35.7–50.0 km in a transect from 33 km to 207 km off the coast of Guangdong Province (China) during spring (April 24–26th, 2013; April 13–16th, 2014) and summer (June 28–30th, 2013; July 27–29th, 2014) on board the R/V Yanping II (**Supplementary Figure S1**). The transect is located between the Taiwan Strait and the SCS. The Taiwan Strait is characterized by a complex bottom topography and is located mostly on the continental shelf with a mean depth of about 60 m. An abrupt depth change is present between the Taiwan Strait and the SCS deep basin, with deepest water depth over 1000 m (Hu et al., 2011). The transect crosses coastal (water depth < 50 m), slope break (water depth < 200 m) and oceanic (water depth up to 1197 m) areas in the northern SCS

(Hu et al., 2011). Sites C1 to C5 are in shallow systems, with depth around 30–60 m (**Supplementary Table S1**). Only surface waters (at a depth of 3 m) were collected. At sites C7 and C9, for which deepest depth are around 130 and 1300 m, respectively, samples were collected at discrete depths (**Supplementary Table S1**). During the study period, a total of 41 samples were collected, with 18 samples from the surface, 16 samples from the euphotic zone (surface layer not included) and 7 samples from the mesopelagic zone (**Supplementary Table S1**). All samples were collected using a conductivity temperature depth (CTD) profiler equipped with 12-l Niskin bottles (SBE 917, United States). The bulk sample was prefiltered through 200  $\mu\text{m}$  nylon mesh (Sefar Nitex) to remove mesozooplanktonic organisms. A subsample (2 L) of the prefiltered water was passed through a 3  $\mu\text{m}$  pore polycarbonate membrane (Millipore, United States), which was then immersed in preservative buffer (RNAlater, Qiagen) and stored at  $-20^{\circ}\text{C}$  until extraction. For the QPS, subsamples (500 ml) of water were collected in spring and summer of the year 2014 from the bulk waters. The samples were fixed immediately with freshly prepared Bouin's preservative according to Montagnes and Lynn (1993).

Temperature, salinity, and depth of all water samples were measured using a conductivity–temperature–depth (CTD) profiler. For chlorophyll *a* analysis, 200 ml seawater was passed through a GF/F filter, which was immediately stored at  $-80^{\circ}\text{C}$  for later extraction (Huang et al., 2010). Acetone was used to extract chlorophyll *a*, the concentration of which was measured by Trilogy fluorometer (Turner Designs, United States). For bacterial abundance analysis, which was only conducted for the samples collected in 2014, 1.8 ml seawater sample was prefiltered onto a 20  $\mu\text{m}$  pore-size membrane and then mixed with ice-cold glutaraldehyde (1% final concentration). Samples were stored at  $-80^{\circ}\text{C}$  and were later measured by a flow cytometry (Beckman Coulter, Epics Altra II) (Jiao et al., 2013). Nutrient analysis (ammonia, nitrite, nitrate, dissolved inorganic nitrogen and phosphate) followed Hu et al. (2008).

## Quantitative Protargol Stain, Nucleic Acid Extraction and PCR

The 22 Bouin's-fixed samples were filtered through a 25 mm diameter 0.8  $\mu\text{m}$  pore-size cellulose nitrate membrane (Sartorius, Lot no: 11404-25), bleached and stained using the QPS (Montagnes and Lynn, 1993). All isolates were observed using an Olympus CX31 microscope under bright field to reveal taxonomically informative features such as the infraciliature and nuclear apparatus. Ciliate identification followed Kofoid and Campbell (1929, 1939) and Song et al. (2009). The abundance of each species was recorded.

In total, 41 samples collected during spring and summer of 2013 and 2014 were processed for HTS of the 18S rRNA gene transcript. For RNA extraction, a RNeasy Mini Kit (Qiagen, United States) was used following the removal of RNAlater buffer (Stoeck et al., 2010). The extracted RNA was treated with the RNase-free DNase set (Qiagen, United States) to remove remaining DNA. Reverse transcription was performed using QuantiTect Reverse Transcription Kit (Qiagen, United States). The PCR amplification of ciliate partial 18S rRNA gene transcript

was performed using ciliate-specific primers (Dopheide et al., 2008). Primers covering the hypervariable V4 region of the 18S rRNA gene transcript were then used in a second PCR following Stoeck et al. (2010). Q5 Hot Start High-Fidelity DNA Polymerase (Cat. #M0493 L, New England Biolabs, United States) was used for fragment amplification. PCR conditions used for the first PCR follows Dopheide et al. (2008) with a few modifications. Details are as follow: an initial incubation for 5 min at  $98^{\circ}\text{C}$  and then 25 cycles of 60 s at  $98^{\circ}\text{C}$  (denaturing), 30 s at  $55^{\circ}\text{C}$  (annealing), and 90 s at  $72^{\circ}\text{C}$  (extension), followed by a final extension step of 7 min at  $72^{\circ}\text{C}$ . PCR conditions used for the second PCR follow Stoeck et al. (2010) with a few modifications. Details are as follows: an initial activation step at  $98^{\circ}\text{C}$  for 5min, followed by 25 three-step cycles consisting of  $98^{\circ}\text{C}$  for 30 s,  $57^{\circ}\text{C}$  for 45 s, and  $72^{\circ}\text{C}$  for 1 min; and a final 7 min extension at  $72^{\circ}\text{C}$ . Each sample was amplified in triplicate, pooled, and purified using the Wizard<sup>®</sup> SV Gel and PCR Clean-Up System (Promega, United States). All purified fragments were paired-end sequenced using Illumina MiSeq platform by the sequencing company Meiji (Shanghai, China). All Illumina MiSeq raw sequence data were deposited in NCBI Sequence Read Archive (accession code PRJNA517357).

## Sequence Data Analyses

Cleaning of raw sequence data was performed with Trimmomatic (Bolger et al., 2014) and Flash (Magoč and Salzberg, 2011), including quality checking and filtering, demultiplexing, and assembly of data. The criteria were as follows: (i) low quality reads that had an average quality score lower than 20 and were shorter than 50 bp were removed; (ii) reads that contained ambiguous characters, a mismatch in barcode and/or two or more mismatches in primer, were discarded; (iii) reads with an overlapping region less than 10 bp, or with a mismatch ratio more than 0.2, were removed. The resulting clean reads were further processed using USEARCH v10 (Edgar, 2010) and were clustered at 97% sequence similarity level. *De novo*-based chimera removal was implemented in the clustering process. UCHIME implemented in USEARCH v10 was used to perform analysis of reference-based chimera removal (Edgar et al., 2011). Representative sequences were then taxonomically assigned against the Protist Ribosomal Reference database v4.7.2 (PR2) by UBLAST (Guillou et al., 2013). Non-ciliate OTUs were manually removed and the generated ciliate-only OTU table was ready for further analyses. Prior to subsequent statistical analyses, the OTU table was rarefied to the same sequencing depth of 7,597 reads per sample by randomly resampling. For samples collected in spring and summer of the year 2014, the OTU table was normalized to 7,532 reads per sample for further analyses.

In order to further explore whether the diversity distribution pattern seen in our study is a general phenomenon, we downloaded HTS data generated from two pilot studies carried out in neighboring oceanic basins, i.e., western Pacific Ocean (Zhao et al., 2017) and eastern North Pacific (Hu et al., 2016), respectively. Both investigations amplified the same hypervariable region, i.e., V4, as that of the present study, derived from HTS of both DNA and cDNA, thus enabling

direct comparisons to be made. Sequence data from the eastern North Pacific were downloaded from the NCBI Sequence Read Archive under accession number SRP070577 (Hu et al., 2016). Sequence data from the western Pacific were downloaded from the NCBI Sequence Read Archive under accession number SRP109014 (Zhao et al., 2017). For the eastern North Pacific, 25 cDNA samples were extracted which encompassed 70,250 ciliate sequences. For the western Pacific, 23 DNA and 6 cDNA samples were extracted which included totals of 739,909 and 202,116 ciliate sequences, respectively. Details of extract locations and depths are given in **Supplementary Table S2**. All data processing was the same as the one dealing with the data from the present study.

## Statistical Analyses

Alpha-diversity estimators were calculated using SPADE (Chao and Shen, 2003) and diversity comparisons on spatial and temporal scales were depicted by boxplots. Sampling sites were defined as nearshore when the water depth was less than 50 m and offshore when the water depth was more than 50 m. To investigate differences between samples, Bray-Curtis distances were calculated and analyzed by Non-Metric Multidimensional Scaling (nMDS) in R using the 'vegan' package<sup>1</sup>. For samples collected in spring and summer of the year 2014, the groupings of samples were identified using PCoA on both morphological and V4 amplicon datasets with the 'vegan' package in R. Global and pairwise differences among groupings of samples were further tested by analysis of similarity (ANOSIM), permutational multivariate analysis of variance (Adonis) and multiple response permutation procedures (MRPP) within R and PRIMER 6 (Clarke and Gorley, 2009). SIMPER analysis was employed to identify those OTUs responsible for the differences observed in the composition across depth strata in PRIMER 6. Indicator species analysis was performed to identify the specific OTUs that characterized each of the ecological layers using the package Indicspecies in R (Dufrene and Legendre, 1997). Only OTUs with indicator values (IV) > 0.3 and  $p < 0.05$  were considered good indicators. The relationships between communities and environmental factors were explored with Mantel tests using the vegan package in R. Partial Mantel tests were used to assess individual effects of depth, geographical distance and environment factors on beta-diversity after controlling for each (Legendre and Legendre, 1998). Quantification of ecological processes, i.e., selection, dispersal and drift, were made according to Stegen et al. (2013) which first uses phylogenetic turnover between communities to determine the influence of selection, then uses OTU turnover to determine the influences of dispersal and drift. Phylogenetic turnover was measured by calculating the weighted  $\beta$ -mean nearest taxon distance ( $\beta$ MNTD), which quantifies the mean phylogenetic distance between the evolutionary closest OTUs in two communities.  $\beta$ MNTD values higher than expected indicate that communities are under heterogeneous selection (Zhou and Ning, 2017). In contrast,  $\beta$ MNTD values which are lower than expected indicate that communities are experiencing homogeneous selection. Null

models were constructed using 999 randomizations as in Stegen et al. (2013). Differences between the observed  $\beta$ MNTD and the mean of the null distribution are denoted as  $\beta$ -Nearest Taxon Index ( $\beta$ NTI).  $\beta$ NTI values higher than 2 or lower than -2 indicate the influence of the deterministic process structuring the community, whereas  $\beta$ NTI values between -2 and 2 indicate the influence of stochastic processes (Stegen et al., 2013). The second step is to calculate whether the observed  $\beta$  diversity, based in OTU turnover, could be generated by drift or other processes. The Raup-Crick metric (Chase et al., 2011) using Bray-Curtis dissimilarities, was calculated following Stegen et al. (2013). RCbray compares the measured  $\beta$  diversity against the  $\beta$  diversity that would be obtained if drift was driving community turnover (i.e., under random community assembly). The randomization was run 999 times. Then the  $\beta$ NTI in combination with RCbray was used to quantify the relative influence of major ecological processes governing the ciliate communities (Stegen et al., 2013).  $\beta$ NTI values higher than 2 or lower than -2 indicate the influence of variable selection and homogeneous selection, respectively. If the  $|\beta$ NTI| is <2 but with an RCbray value lower than -0.95 or higher than +0.95, the community assembly is governed by homogenizing dispersal or dispersal limitation, respectively. In addition, a  $|\beta$ NTI| of <2 and a |RCbray| of <0.95 suggest that the community assembly is not dominated by any single process (Stegen et al., 2013).

## RESULTS

### Environmental Parameters

Environmental parameters collected along the transect showed gradients in both dimensions, i.e., horizontally from coastal to oceanic waters and vertically from surface to deep waters. Variations occurring horizontally along the transect were linked mainly to increases in temperature and salinity and a decrease in turbidity from coastal to oceanic waters, whereas variations occurring vertically down the water column were linked to a decrease in temperature and increases in pressure, salinity, and concentrations of nitrate, phosphate and dissolved inorganic nitrogen, from surface to deep waters (**Table 1** and **Supplementary Figure S1**). Environmental factors such as temperature, salinity, pressure, dissolved oxygen, pH, abundances of bacteria and concentration of nutrients co-varied significantly with water depth (**Supplementary Table S3**), suggesting strong vertical variability in environmental features. In addition, the interface (100–200 m) between the euphotic and mesopelagic zones is highly heterogeneous, and represents a layer of major transitions of several factors, i.e., concentrations of dissolved oxygen, nitrite, nitrate, phosphate and dissolved inorganic nitrogen, temperature, turbidity and pH (**Table 1**). For ease of description, terms used to describe water layers at different depths are defined here. Water at the depth of 3 m is defined as surface; water between 50 and 100 m is defined as euphotic zone; water between 200 and 1000 m is defined as mesopelagic zone; water between 100 and 200 m is defined as transitional zone, i.e., the layer between the base of the euphotic zone and the top of the mesopelagic zone.

<sup>1</sup><http://vegan.r-forge.r-project.org/>

**TABLE 1** | Environmental parameters at sampling sites throughout period of study (mean  $\pm$  SD).

Sampling sites	C1 3 m	C3 3 m	C5 3 m	C7 3 m	C9 3 m	C7 50–100 m	C9 50–100 m	C9 200 m	C9 1000 m
Salinity (‰)	33.21 $\pm$ 1.28	32.93 $\pm$ 1.52	33.58 $\pm$ 0.64	33.77 $\pm$ 0.34	33.92 $\pm$ 0.35	34.43 $\pm$ 0.22	34.37 $\pm$ 0.24	34.52 $\pm$ 0.01	34.56 $\pm$ 0.04
Temperature (°C)	25.06 $\pm$ 2.00	26.90 $\pm$ 3.29	27.22 $\pm$ 2.85	27.32 $\pm$ 2.02	27.36 $\pm$ 2.16	21.34 $\pm$ 3.45	23.54 $\pm$ 2.39	15.22 $\pm$ 1.17	4.36 $\pm$ 0.44
DO (mg/L)	6.83 $\pm$ 0.28	6.67 $\pm$ 0.61	6.50 $\pm$ 0.59	6.23 $\pm$ 0.21	6.63 $\pm$ 0.28	5.79 $\pm$ 0.53	5.70 $\pm$ 0.51	3.92 $\pm$ 0.65	3.23 $\pm$ 0.13
Pressure (db)	3.69 $\pm$ 1.16	3.52 $\pm$ 1.01	3.52 $\pm$ 1.01	3.69 $\pm$ 1.16	3.03 $\pm$ 0.02	79.62 $\pm$ 29.88	72.32 $\pm$ 24.94	201.30 $\pm$ 0.11	1008.60 $\pm$ 0.55
pH	8.46 $\pm$ 0.13	8.39 $\pm$ 0.17	8.39 $\pm$ 0.17	8.47 $\pm$ 0.12	8.33 $\pm$ 0.08	8.34 $\pm$ 0.15	8.27 $\pm$ 0.07	8.13 $\pm$ 0.06	7.86 $\pm$ 0.06
Turbidity (FTU)	1.33 $\pm$ 1.26	0.80 $\pm$ 0.29	0.61 $\pm$ 0.00	0.50 $\pm$ 0.10	0.50 $\pm$ 0.04	0.58 $\pm$ 0.04	0.53 $\pm$ 0.08	0.26 $\pm$ 0.10	0.61 $\pm$ 0.00
Chl <i>a</i> ( $\mu$ g/L)	1.51 $\pm$ 0.99	0.34 $\pm$ 0.20	0.13 $\pm$ 0.02	0.13 $\pm$ 0.09	0.11 $\pm$ 0.06	0.24 $\pm$ 0.19	0.35 $\pm$ 0.17	0.02 $\pm$ 0.04	0.00 $\pm$ 0.00
Bacteria ( $10^4$ cells/mL)	136.15 $\pm$ 4.95	107.44 $\pm$ 29.10	103.24 $\pm$ 38.76	91.45 $\pm$ 32.76	70.96 $\pm$ 11.16	68.23 $\pm$ 37.41	54.61 $\pm$ 19.62	23.65 $\pm$ 2.17	8.70 $\pm$ 3.70
DIN (mg/L)	0.016 $\pm$ 0.003	0.010 $\pm$ 0.010	0.014 $\pm$ 0.008	0.024 $\pm$ 0.019	0.016 $\pm$ 0.012	0.060 $\pm$ 0.033	0.047 $\pm$ 0.041	0.158 $\pm$ 0.019	0.416 $\pm$ 0.058
NO <sub>2</sub> (mg/L)	0.002 $\pm$ 0.002	0.002 $\pm$ 0.002	0.002 $\pm$ 0.002	0.001 $\pm$ 0.001	0.001 $\pm$ 0.001	0.002 $\pm$ 0.001	0.003 $\pm$ 0.003	0.001 $\pm$ 0.001	0.001 $\pm$ 0.001
NO <sub>3</sub> (mg/L)	0.012 $\pm$ 0.006	0.006 $\pm$ 0.010	0.008 $\pm$ 0.008	0.017 $\pm$ 0.014	0.013 $\pm$ 0.011	0.055 $\pm$ 0.035	0.043 $\pm$ 0.041	0.154 $\pm$ 0.016	0.409 $\pm$ 0.054
NH <sub>4</sub> (mg/L)	0.002 $\pm$ 0.003	0.003 $\pm$ 0.006	0.004 $\pm$ 0.004	0.006 $\pm$ 0.005	0.002 $\pm$ 0.003	0.003 $\pm$ 0.005	0.002 $\pm$ 0.002	0.002 $\pm$ 0.003	0.006 $\pm$ 0.003
PO <sub>4</sub> (mg/L)	0.003 $\pm$ 0.003	0.002 $\pm$ 0.002	0.002 $\pm$ 0.002	0.003 $\pm$ 0.003	0.005 $\pm$ 0.003	0.011 $\pm$ 0.006	0.010 $\pm$ 0.009	0.028 $\pm$ 0.003	0.079 $\pm$ 0.007

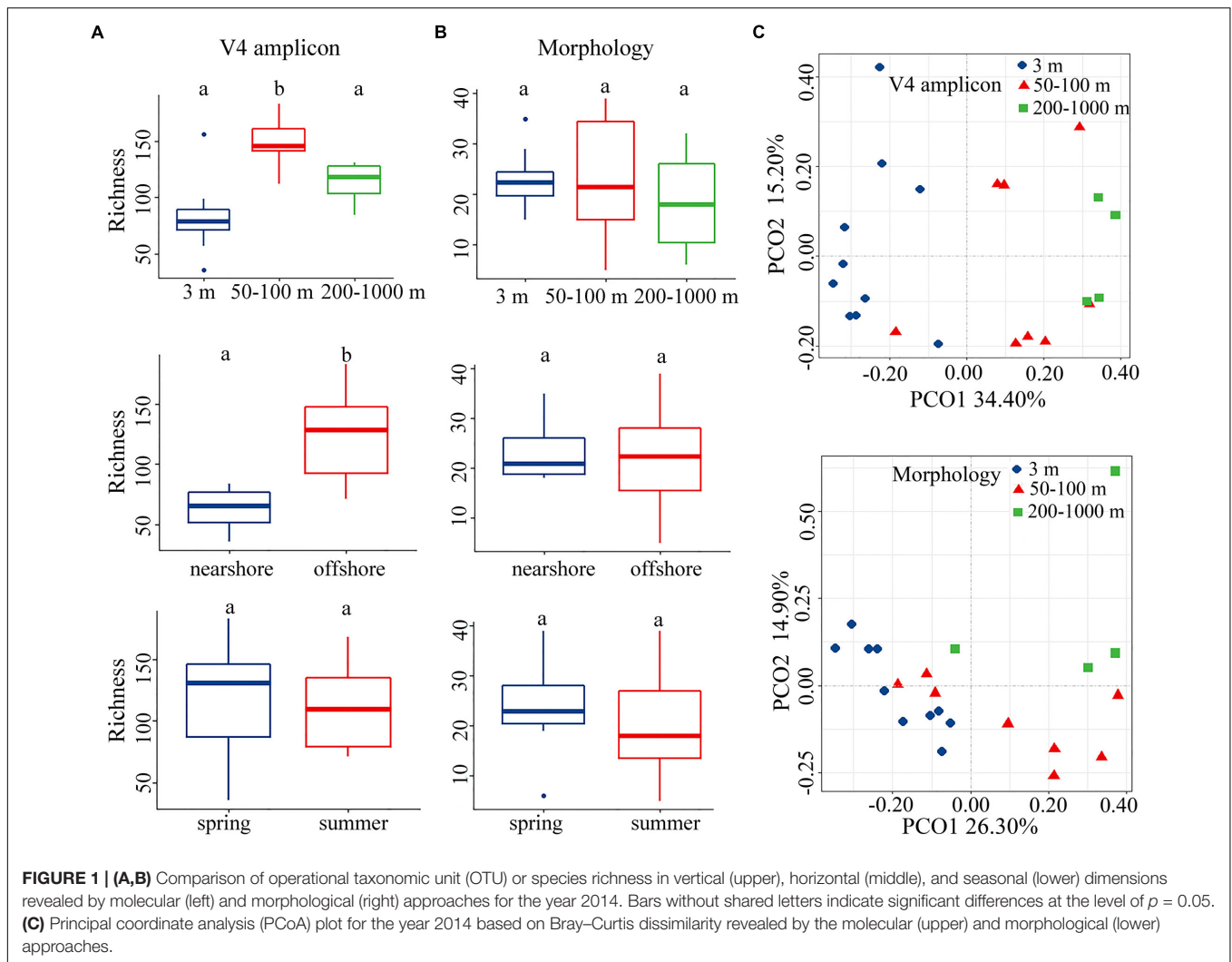
DO and pH were not measured for samples collected in the summer of 2013, and bacteria were not enumerated for samples collected in the spring and summer of 2013.

## Diversity Distribution and Community Structure of Ciliates Revealed by Both Morphology and rRNA Gene Transcript Datasets (Year 2014)

### Alpha- and Beta-Diversity Distribution Patterns and Their Relations to Spatial and Temporal Variations

We compared distribution patterns, rather than the exact values, of alpha-diversity using two approaches, i.e., morphology and rRNA gene transcripts. In contrast to morphospecies richness, OTU richness had a clear spatial distribution, both horizontally and vertically (**Figures 1A,B**, upper and middle). When samples were considered by ecological layers (surface, euphotic zone, and mesopelagic zone), there was a marked increase of OTU richness from the surface to the euphotic waters (**Figure 1A**, upper and **Supplementary Table S4**). Both approaches revealed that the mesopelagic zone possessed comparable diversity to that of surface layer (**Figures 1A,B** and **Supplementary Table S4**), with higher diversity occurring on the top of the mesopelagic zone (**Supplementary Figures S2a,b**), which was consistent with the result from the pooled data for the years 2013 and 2014 (**Supplementary Figure S3a**). This vertical distribution pattern of alpha-diversity was consistent over seasonal and annual timescales. In contrast to the clear spatial distribution, differences of alpha-diversity between seasons (spring-summer) were statistically insignificant (**Figures 1A,B**, lower and **Supplementary Table S4**). This was consistent with the results from the pooled data for the years 2013 and 2014 which showed that ciliate alpha-diversity had a clear spatial, but no temporal, distribution pattern (**Supplementary Figure S3b**).

Both morphological and molecular approaches captured similar vertical distribution patterns of ciliate communities based on PCoA, ANOSIM, Adonis and MRPP analyses, identifying three ciliate assemblages that were mainly grouped by water depth, i.e., the surface, euphotic, and mesopelagic zones groups (**Figure 1C** and **Table 2**). SIMPER analysis showed that there are two major contributors to the vertical community rearrangements, i.e., Spirotrichea (which contributed 29.05 and 62.03% to the molecular and morphological datasets, respectively) and Oligohymenophorea (which contributed 27.57 and 21.62% to the molecular and morphological datasets, respectively). Although the relative sequence abundance of spirotricheans declined with depth from surface to euphotic zone in both datasets, it increased from the euphotic to mesopelagic zones in the molecular dataset but decreased in the morphological dataset (**Supplementary Table S5**). The relative sequence abundance of oligohymenophoreans increased with depth in both datasets (**Supplementary Table S5**). In addition, we observed a change in indicator species in different ecological layers, e.g., OTUs 1, 26, and 46, which showed a high similarity to an environmental ciliate sequence (KJ763408, coverage 100%, similarity 100%), *Amphorellopsis* sp. (KF130398, coverage 100%, similarity 100%), and *Eutintinnus fraknoi* (JQ408159, coverage 100%, similarity 99%), respectively, made a high contribution to the surface water communities. By contrast, OTUs 38, 64, 103, and 89, which were closely related to an uncultured eukaryote sequence from a high-Arctic fjord, Isfjorden in West



Spitsbergen, Norway (KT810411, coverage 98%, similarity 99%), an uncultured deep sea (1500–2500 m) eukaryote sequences from East Pacific Rise, North Pacific (KJ761209, KJ760912, KJ757205, coverage 100%, similarity 100%), an uncultured eukaryote sequences from coastal North Pacific (KJ762665, coverage 100%, similarity 99%) and a Gulf Stream, North Atlantic (KJ760065, coverage 100%, similarity 99%), and an uncultured apistome ciliate (JX417930, coverage 100%, similarity 100%), respectively, dominated the mesopelagic zone (Figure 2). The community structure in both the surface and euphotic zones exhibited seasonal changes (Table 2). The molecular dataset also revealed the presence of a distance-decay pattern in the community composition from coastal to oceanic waters (Table 2). By contrast, although the morphological dataset revealed a significant difference in community composition between spring and summer, it failed to detect a nearshore-offshore distribution pattern (Table 2). Beta-diversity based on the pooled rRNA dataset for the years 2013 and 2014 also captured a clear spatial, but no temporal distribution pattern (Supplementary Table S6).

Spirotrichea and Oligohymenophorea dominated ciliate communities from the surface down to mesopelagic zone in

the morphological dataset in the year 2014 (Supplementary Figure S4a), with the former contributing higher sequence abundance to the communities than that of the latter at the surface and in the euphotic zone whereas in the mesopelagic zone the opposite was true (Supplementary Figure S4a). Together with Phyllopharyngea, these two classes were significant contributors to the ciliate communities across three depth strata, i.e., surface, euphotic and mesopelagic zones, in the molecular dataset in the year 2014 (Supplementary Figure S4b), reflecting the results of the pooled dataset for the years 2013 and 2014 (Supplementary Figure S4b). Spirotricheans, the largest representatives in the ciliate communities, decreased from surface to euphotic zone in both morphological and molecular datasets (Supplementary Figures S4a–c). Spirotrichea remained the dominant class in the mesopelagic zone in the molecular dataset in the year 2014 (Supplementary Figure S4b). By contrast, Oligohymenophorea was the dominant class below the euphotic zone in the morphological dataset in the year 2014 (Supplementary Figure S4a) and in the pooled dataset for years 2013 and 2014 (Supplementary Figure S4c). The relative contributions of Oligohymenophorea and Phyllopharyngea to

**TABLE 2** | ANOSIM, Adonis, and MRPP statistical tests of the groupings of molecular- and morphology-based ciliate communities according to depth, region and season.

	ANOSIM						Adonis						MRPP							
	2014_V4		2014_Morphology		2014_V4		2014_Morphology		2014_V4		2014_Morphology		2014_V4		2014_Morphology		2014_V4		2014_Morphology	
	R	P	R	P	R <sup>2</sup>	P	R <sup>2</sup>	P	R <sup>2</sup>	P	R <sup>2</sup>	P	A	P	A	P	A	P	A	
Depth (N = 22)	0.66	<0.001	0.392	<0.001	0.375	0.001	0.25	0.001	0.169	0.001	0.088	0.001	0.169	0.001	0.088	0.001	0.169	0.001	0.088	
3 m vs. 50–100 m (N(3 m) = 10, N(50–100 m) = 8)	0.6	<0.001	0.288	0.002	0.284	0.002	0.143	0.006	0.13	0.001	0.047	0.006	0.13	0.001	0.047	0.006	0.13	0.001	0.047	
3 m vs. 200–1000 m (N(3 m) = 10, N(200–1000 m) = 4)	0.879	0.002	0.66	0.004	0.353	0.002	0.277	0.002	0.157	0.002	0.105	0.002	0.157	0.002	0.105	0.002	0.157	0.002	0.105	
50–100 m vs. 200–1000 m (N(50–100 m) = 8, N(200–1000 m) = 4)	0.572	0.008	0.276	0.072	0.259	0.008	0.195	0.022	0.096	0.003	0.06	0.022	0.096	0.003	0.06	0.022	0.096	0.003	0.06	
Nearshore vs. offshore (N(nearshore) = 4, N(offshore) = 18)	0.353	0.008	−0.038	0.531	0.138	0.003	0.06	0.153	0.052	0.005	0.012	0.153	0.052	0.005	0.012	0.153	0.052	0.005	0.012	
Season (spring vs. summer) (N(spring) = 11, N(summer) = 11)	0.021	0.273	0.126	0.019	0.056	0.243	0.084	0.046	0.007	0.227	0.02	0.046	0.007	0.227	0.02	0.046	0.007	0.227	0.02	
Spring vs. summer (3 m) (N(spring) = 5, N(summer) = 5)	0.188	0.077	0.556	0.007	0.178	0.143	0.252	0.009	0.031	0.088	0.082	0.009	0.031	0.088	0.082	0.009	0.031	0.088	0.082	
Spring vs. summer (50–100 m) (N(spring) = 4, N(summer) = 4)	0.056	0.347	0.135	0.196	0.184	0.129	0.151	0.272	0.041	0.088	0.002	0.272	0.041	0.088	0.002	0.272	0.041	0.088	0.002	

Community turnover is based on the Bray–Curtis distance. Numbers in bold indicate statistically significant results.

ciliate communities down the water column showed opposite trends, that of the former increasing with water depth in all datasets (**Supplementary Figures S4a–c**) whereas that of the latter decreasing with water depth in molecular datasets (**Supplementary Figures S4b,c**).

### Determinants of Ciliate Community Dynamics

Depth, geographic distance and environmental factors were generally correlated with ciliate beta-diversity, the only exception being that between geographic distance and community variation in the morphological dataset (**Table 3**). The partial Mantel test revealed that depth made a greater contribution to community variation, with higher R values of depth (ranging from 0.485 to 0.593) than those of geographic distance (from 0.370 to 0.395) and environment (from 0.004 to 0.414) (**Table 3**). These results were also reflected in the plots of depth, geographic distance and environmental heterogeneity versus community dissimilarity, all of which had positive slopes, with depth showing the highest correlation (**Supplementary Figures S5a–c**). Depth and environmental factors explained both molecular- and morphology-based ciliate community variability, with statistically significant relationships occurring more frequently for OTUs than for morphospecies (**Table 3**). Statistically significant results were revealed for depth after controlling for environmental factors, while all putatively correlated factors showed either a decrease in correlation coefficient or an insignificant effect on morphology-based beta-diversity when depth was controlled (**Table 3**).

To further assess the contributions of spatial and environmental factors on ciliate community structure, quantification of the ecological processes mediating community assembly was performed with the phylogenetic null model analysis (**Figure 3**). It was found that dispersal limitation, which generates divergence in community composition due to limited exchange of microbes, was primary for total community and explained 47.2% of community turnover (**Figure 3**). Although the combined effects of non-selection processes explained more of the variation of the surface community, heterogeneous selection itself, which causes community composition to be dissimilar under variable environmental conditions, explained 44.4% of the variation. For euphotic and mesopelagic zones, dispersal limitation (51.7 and 57.1%, respectively) and heterogeneous selection (30.8 and 33.3%, respectively) were the major contributors to community turnover, while ecological drift which results from population sizes fluctuating due to chance events, contributed 17.5 and 9.5%, respectively (**Figure 3**). Considering the high ciliate diversity in the transitional layer, the processes shaping community assembly in this layer were also analyzed. In contrast to the other layers, heterogeneous selection contributed 57.8% of community variation, whereas dispersal limitation and ecological drift explained only 28.9 and 13.3% of the variation (**Figure 3**).

### Ciliate Taxonomy and Abundance Revealed by QPS

In total, 79 morphospecies were recovered based on QPS analysis, representing 29 genera, 23 families, 9 orders, 7

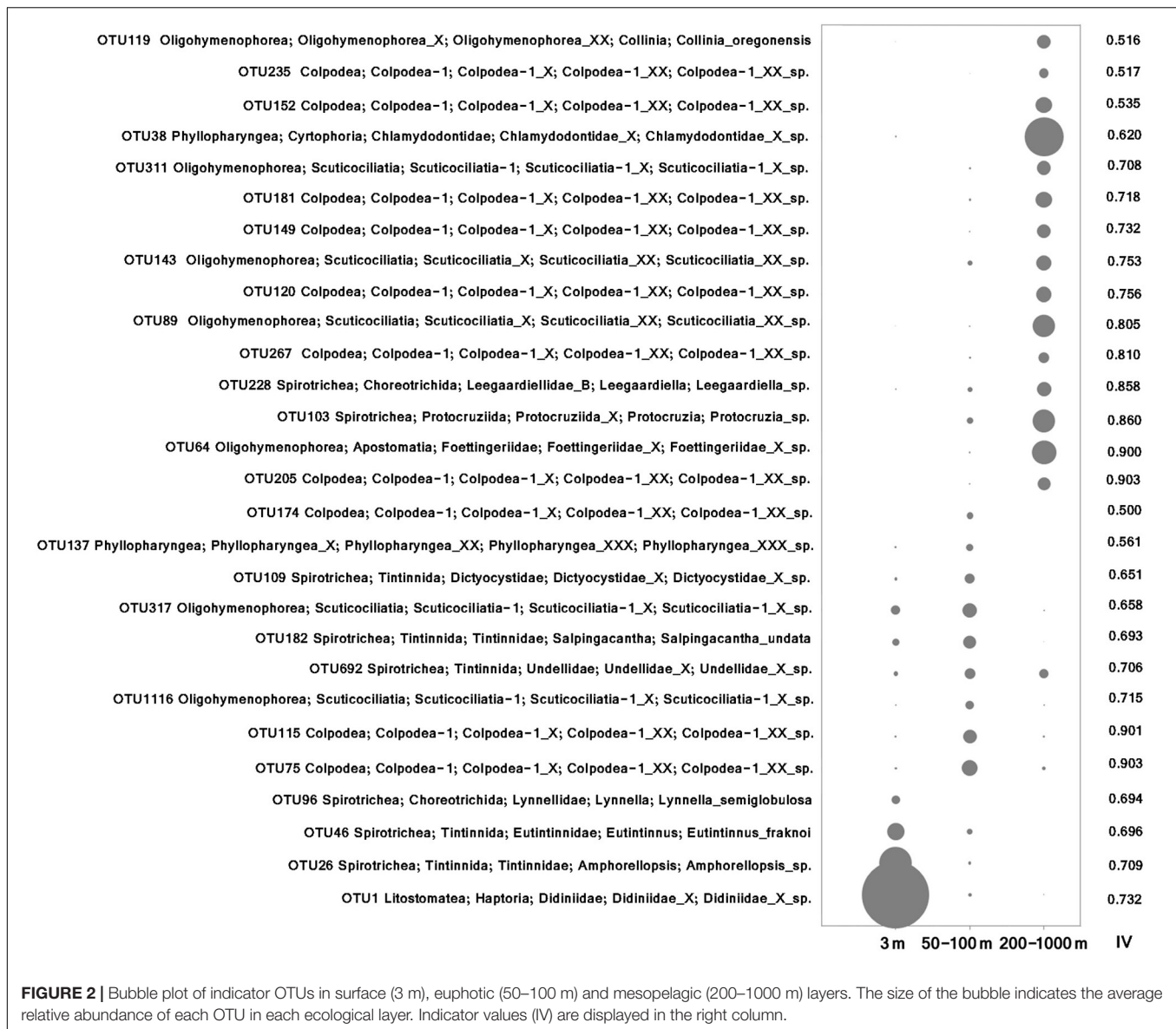


**FIGURE 2** | Bubble plot of indicator OTUs in surface (3 m), euphotic (50–100 m) and mesopelagic (200–1000 m) layers. The size of the bubble indicates the average relative abundance of each OTU in each ecological layer. Indicator values (IV) are displayed in the right column.

subclasses and 5 classes (**Supplementary Table S7**). Among the seven subclasses, species of Oligotrichia (31.33%), Choreotrichia (28.35%), Scuticociliatia (19.77%) and Haptoria (16.32%) contributed over 95% of the total abundance. The most abundant subclass, the aloricate Oligotrichia, showed great diversity in terms of morphology (**Figure 4**). Several isolates appear to be new to science given the combination of their unique infraciliature and minute body size (10–20  $\mu\text{m}$ ). These will be reported in detail in a separate taxonomic paper. At order and family ranks, members of Strombidiida and Strombidiidae had the highest abundances, accounting for 31.32% and 30.75% of the total abundance, respectively. *Strombidium* was the most abundant genus among the 29 genera recovered, contributing 30.72% of the total abundance. The three most abundant species were from classes Haptoria and Spirotrichea, i.e., a species of Didiniidae (8.74%), a species of Tontoniidae (6.48%) and

*Strombidium* sp5 (6.42%), collectively contributing 21.64% of the total ciliate abundance.

In spring and summer of 2014, average ciliate abundances in surface waters were 2,120 ind/L and 1,509 ind/L, respectively, as revealed by QPS. In both seasons, the inshore average abundances (on average 2,006 ind/L in spring and 1,366 ind/L in summer) of ciliates in surface waters were lower than those offshore (on average 2,290 ind/L in spring and 1,723 ind/L in summer) (**Supplementary Figure S6**). Vertically, the maximum abundance of ciliates occurred at 50 m at all offshore sites, with 5,451 ind/L at C7-50m in spring and 3,533 ind/L at C9-50 m in summer (**Supplementary Figure S6**). The minimum abundances all appeared at 1000 m of C9 in both seasons (**Supplementary Figure S6**).

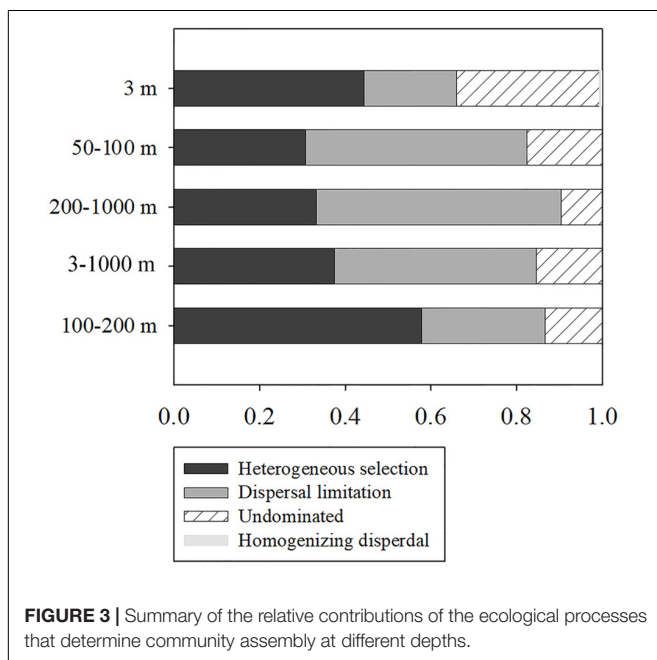
As depth was the most influential factor for community variability, the dominant species above and below photic zone



**TABLE 3** | Simple and partial Mantel tests for the correlations between spatial/environmental factors and ciliate communities revealed by the rRNA gene transcript and morphology datasets for the year 2014.

Mantel test	2014_V4		2014_morphology		Partial Mantel test control for	2014_v4		2014_Morphology	
	R	P	R	P		R	P	R	P
Depth	0.585	<0.001	0.41	<0.001	Geo_distance	0.593	<0.001	0.384	<0.001
					Environment	0.485	<0.001	0.296	<0.001
Geo_distance	0.426	<0.001	0.086	0.242	Depth	0.37	0.001	0.056	0.3
					Environment	0.395	<0.001	0.01	0.422
Environment	0.380	<0.001	0.241	0.039	Depth	0.004	0.434	-0.0001	0.457
					Geo_distance	0.414	<0.001	0.261	0.029
Pressure	0.585	<0.001	0.41	<0.001	Depth	-0.147	0.941	-0.19	0.965
Temperature	0.385	0.006	0.345	0.045	Depth	0.258	0.014	0.134	0.161
Salinity	0.357	0.004	0.007	0.393	Depth	0.216	0.041	-0.18	0.939
Turbidity	0.033	0.349	-0.072	0.646	Depth	0.053	0.31	-0.113	0.769
Chl a	0.096	0.203	0.013	0.364	Depth	0.052	0.283	-0.081	0.71
Bacteria	0.537	<0.001	0.426	0.007	Depth	0.267	0.004	0.124	0.143
DIN	0.410	0.003	0.425	0.015	Depth	0.104	0.198	0.247	0.051
NO <sub>2</sub>	-0.017	0.524	-0.173	0.963	Depth	0.119	0.097	-0.097	0.851
NO <sub>3</sub>	0.412	0.003	0.425	0.017	Depth	0.114	0.169	0.23	0.063
NH <sub>4</sub>	-0.04	0.656	0.079	0.192	Depth	-0.048	0.699	0.078	0.176
PO <sub>4</sub>	0.410	0.001	0.368	0.025	Depth	0.197	0.048	0.199	0.072

Numbers of samples for statistical analyses are 22. Numbers in bold indicate statistically significant results.



were also analyzed. The same three species that dominated species abundance of the total community also dominated the photic zone, i.e., a species of Didiniidae (8.89%), a species of Tontoniidae (6.54%) and *Strombidium* sp5 (6.35%), which collectively contributed 21.78% of the abundance in waters of the 3–100 m depth range. In the aphotic zone, *Strombidium* sp5 (9.25%) and two species of Scuticociliatia (7.09 and 6.89%,

respectively) were the three most abundant species, collectively contributing 23.23% of ciliate abundance in waters of the 200–1000 m depth range. Interestingly, *Strombidium* sp5 was found to be one of the three most abundant species in both the photic and the aphotic zones.

The ciliate community also showed seasonal variation (Table 2) so the dominant species in spring and summer were analyzed. The same three species that dominated species abundance of the total community also dominated the spring community, i.e., a species of Didiniidae (9.94%), a species of Tontoniidae (8.14%) and *Strombidium* sp5 (7.20%), which collectively contributed 25.28% of the abundance in spring community. In summer, a species of Didiniidae (6.63%), a species of Scuticociliatia (5.48%) and *Leegaardiella ovalis* (5.34%) were the three most abundant species, collectively contributing 17.45% of ciliate abundance.

## Mesopelagic Ciliates Across Oceanic Basins

Both morphological and molecular approaches showed that the mesopelagic ciliates possessed comparable diversity to that of the surface layer in the northern SCS (Figures 1A,B upper). To further test how this diversity distribution related to spatial changes, datasets from the western Pacific Ocean (Zhao et al., 2017) and eastern North Pacific (Hu et al., 2016) were analyzed. These revealed a consistent distribution pattern in each of the three oceanic basins regardless of the type of dataset analyzed, i.e., rRNA gene, rRNA gene transcript or morphology (Figures 5A–C). Generally, alpha diversity indices (richness, phylogenetic diversity and Shannon)

of mesopelagic ciliates across oceanic basins showed insignificant differences, except for the eastern North Pacific vs. the western Pacific Ocean regarding phylogenetic diversity (**Figure 6A** and **Supplementary Table S8**). About 12.80–38.98% of all OTUs in the mesopelagic dataset were unique to each oceanic region (**Figure 6B**). Among the total of 703 OTUs, 11.81% were shared by all three basins, whereas OTUs shared by any two basins accounted for 1.99–15.08%, that between the northern SCS and the eastern North Pacific being lowest (**Figure 6C**). PCoA revealed that mesopelagic samples from different oceanic basins were clearly separated from each other in their community composition (**Figure 6D**). The analysis of the global R statistics by the ANOSIM demonstrated that differences in mesopelagic ciliate communities between oceanic basins were significantly different. In addition, pairwise comparisons of the mesopelagic ciliate communities clearly indicated that oceanic basins differed from each other, although the difference between the two neighboring basins, i.e., northern SCS and western Pacific Ocean, was lower than other pairwise comparisons (**Supplementary Table S9**). Phylogenetic null model analysis showed that heterogeneous selection was responsible for 51.26% of compositional variation of mesopelagic ciliate communities across basins, whereas ecological drift and dispersal limitation accounted for 33.10 and 13.79% of community variation, respectively (**Figure 6B**).

## DISCUSSION

### Diversity Distribution of Ciliates in Mesopelagic Waters Across Spatiotemporal Scales

Although studies on ciliate distribution down the water column, especially below the euphotic zone, are limited, different distribution patterns of alpha-diversity have previously been reported (Tanaka and Rassoulzadegan, 2002; Countway et al., 2010; Wickham et al., 2011; Grattepanche et al., 2016). A microscopy-based study showed low biomass and abundance of ciliates below the euphotic zone in the northwestern Mediterranean Sea (Tanaka and Rassoulzadegan, 2002). Likewise, the ciliate alpha-diversity declined with depth less steeply than biomass and abundance below the euphotic zone in the Amundsen and Bellingshausen Seas (Wickham et al., 2011). Using clone libraries, a lower abundance of ciliate OTUs was found in the waters below than above the euphotic zone in North Pacific Ocean, with alpha-diversity decreasing with increasing depth (Countway et al., 2010). By contrast, using pyrosequencing of rRNA genes, alpha-diversity increased with increasing depth for oligotrichians and choreotrichians, with the highest diversity occurring below the euphotic zone along a 163 km transect off the coast of New England, United States (Grattepanche et al., 2016). In the present study, we observed neither a decrease nor an increase of alpha-diversity in the mesopelagic zone. Rather, the rRNA gene transcript-based data revealed that the mesopelagic zone possessed comparable diversity to that of the surface (**Figure 1A** and **Supplementary**

**Figure S3a**). This finding was mirrored by the morphology-based data (**Figure 1B**). The sharp contrast between consistent patterns shown here and the lack of consistent patterns in previous studies could be due to methodological differences and/or local characteristics of the different oceanic regions. HTS methods have recently been developed which can detect species even if present in low number, thereby avoiding the bias that leads to underestimates the diversity of small, cryptic and low abundance species using morphology-based and classical molecular-based methods (Santoferrara et al., 2014). Previous studies investigating temporal changes in species richness and abundance of mesopelagic tintinnids in the North West Mediterranean Sea (Dolan et al., 2019), and in biomass of mesopelagic ciliates in the Arabian Sea (Gowing et al., 2003) have yielded contrasting findings which likely reflected differences in the two ecosystems examined. The mesopelagic zone is not uniform, but contains a strong gradient of environmental factors, especially at the interface with the euphotic zone (Dehairs et al., 1997; Robinson et al., 2010). These environmental gradients may support a wide range of niches that can be occupied by organisms with different functionality. Furthermore, the steep environmental gradients, both physical and chemical, may prevent strong dominance by any particular species, thus helping to create biodiversity hotspots. This is exemplified by the significantly lower ciliate abundance, but comparable alpha diversity, in the mesopelagic zone compared to the surface (**Figure 1B** and **supplementary Figure S6**).

### Ciliate Community Structure and Assembly Mechanisms Across Depth Strata

There are marked biochemical and physical gradients down the water column from the surface to the mesopelagic zone. This provides a structured environment and generates different ecological layers, leading to strong dispersal limitation and environmental selection among layers and within each layer. Different ciliate assemblages are associated with these ecological layers and two classes in particular, Spirotrichea and Oligohymenophorea, contributed significantly to differences among the vertical communities (**Supplementary Table S5**). In the case of Spirotrichea (mainly Oligotrichia and Choreotrichia), abundance of OTUs affiliated to loricate choreotrichs (tintinnids) was lower in the mesopelagic zone (14.84%) than in layers above (18.72%) whereas oligotrichs together with aloricate choreotrichs showed an opposite trend (82.81% in mesopelagic vs. 77.02% in layers above). This is mirrored by morphological data that showed the relative abundance of loricate choreotrichs was lower in the mesopelagic zone (13.28%) than in layers above (20.23%) whereas the relative abundance of oligotrichs together with aloricate choreotrichs was higher in mesopelagic (86.72%) than in layers above (78.84%). Further analysis showed that loricate and aloricate ciliates accounted for 32.35% and 66.29% of spirotrichean community variations, respectively. Prey was found to be an important beta-diversity driver of tintinnid communities across the shelf off the coast of Rhode Island (United States) and small-sized tintinnids were proposed to

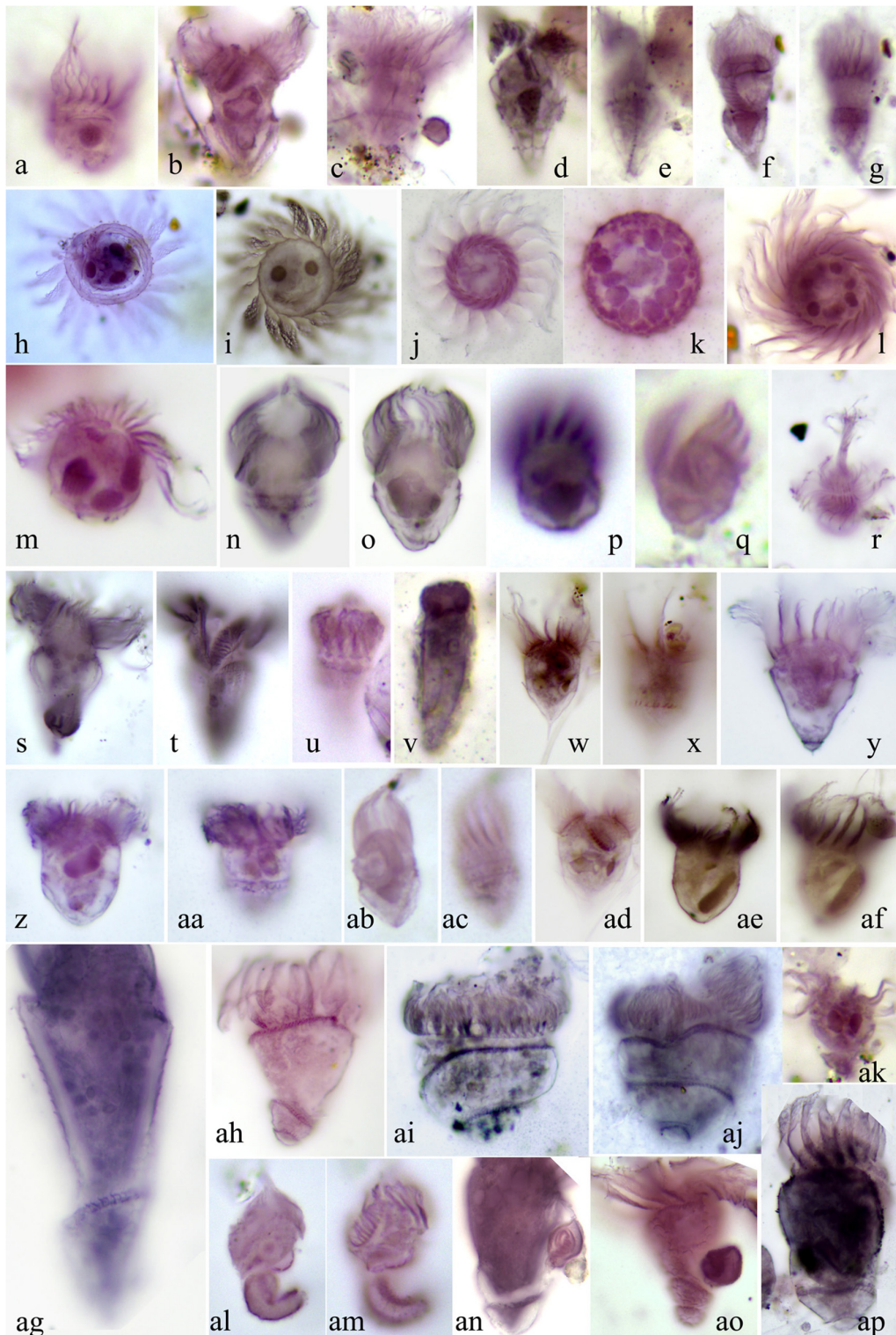


**FIGURE 4** | Morphology of representative oligotrichians and aloricate choreotrichians following protargol staining. **(a)** *Leegaardiella ovalis*. **(b,c)** *Strombidium bilobum*. **(d,e)** *Strombidium dalum* sensu Lynn et al. (1988). **(f,g)** *Strombidium emergens*. **(h)** *Leegaardiella cf. sol.* **(i)** *Leegaardiella sol.* **(j-l)** *Rimostrombidium multinucleatum*. **(m)** *Lohmanniella* sp2. **(n,o)** *Strombidium* sp3. **(p,q)** *Strombidium pollostomum*. **(r)** *Mesodinium* sp. **(s,t)** *Pseudotontonia cornuta*. **(u,v)** *Strombidinopsis* sp. **(w,x,ad)** *Strombidium styliferum*. **(y)** *Strombidium constrictum*. **(z,aa)** *Strombidium cf. inclinatum*. **(ab,ac)** *Strombidium dalum*. **(ae,af)** *Strombidium* sp4. **(ag)** *Loboaea strobila* Lohmann, 1908. **(ah)** *Loboaea* sp. **(ai,aj)** *Parallelostrombidium kahli*. **(ak)** Tontoniidae sp. **(al,am)** *Paratontonia gracillima*. **(an)** *Spirotontonia turbinata*. **(ao)** *Spirotontonia grandis*. **(ap)** *Spirotontonia* sp.

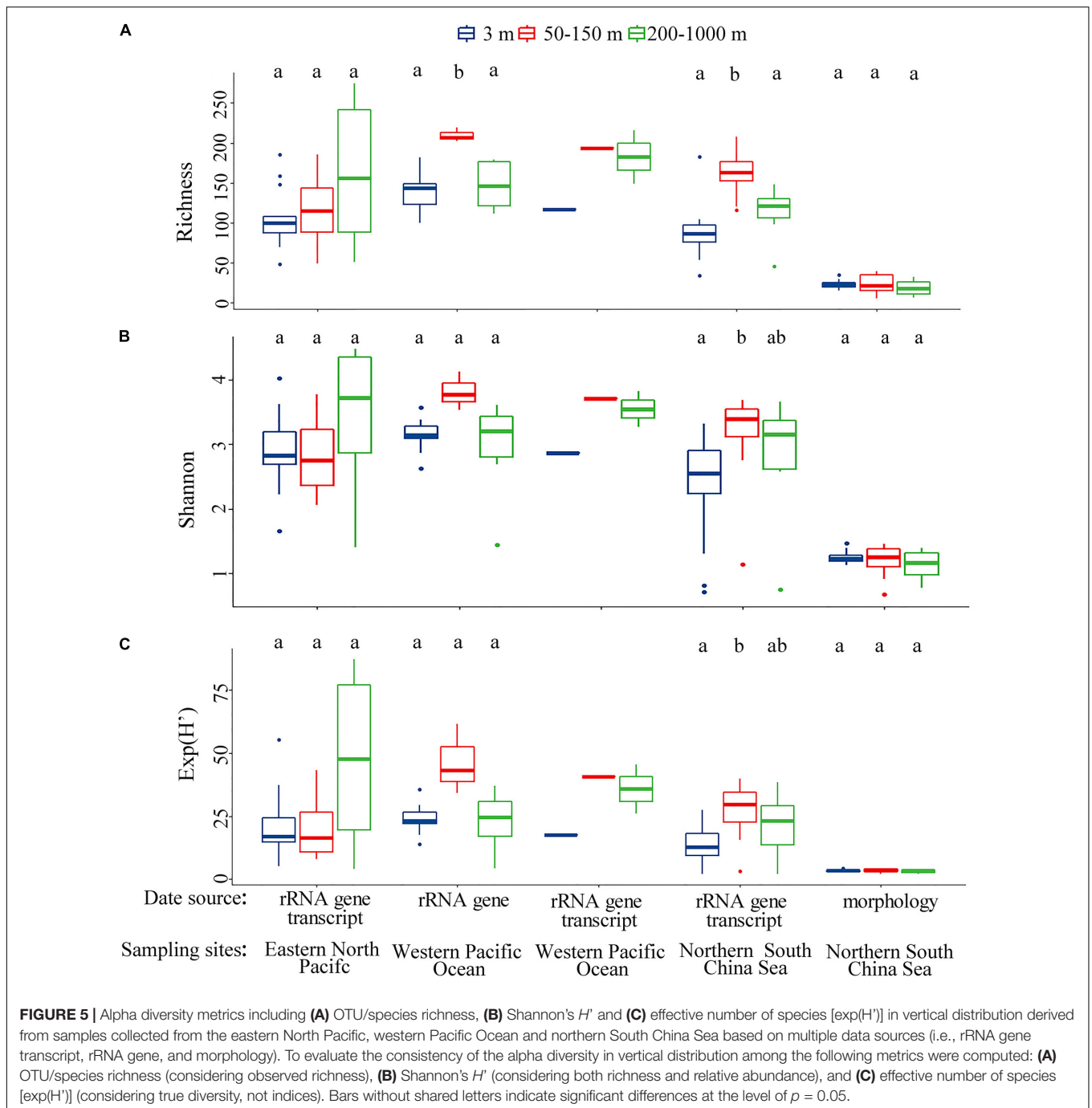
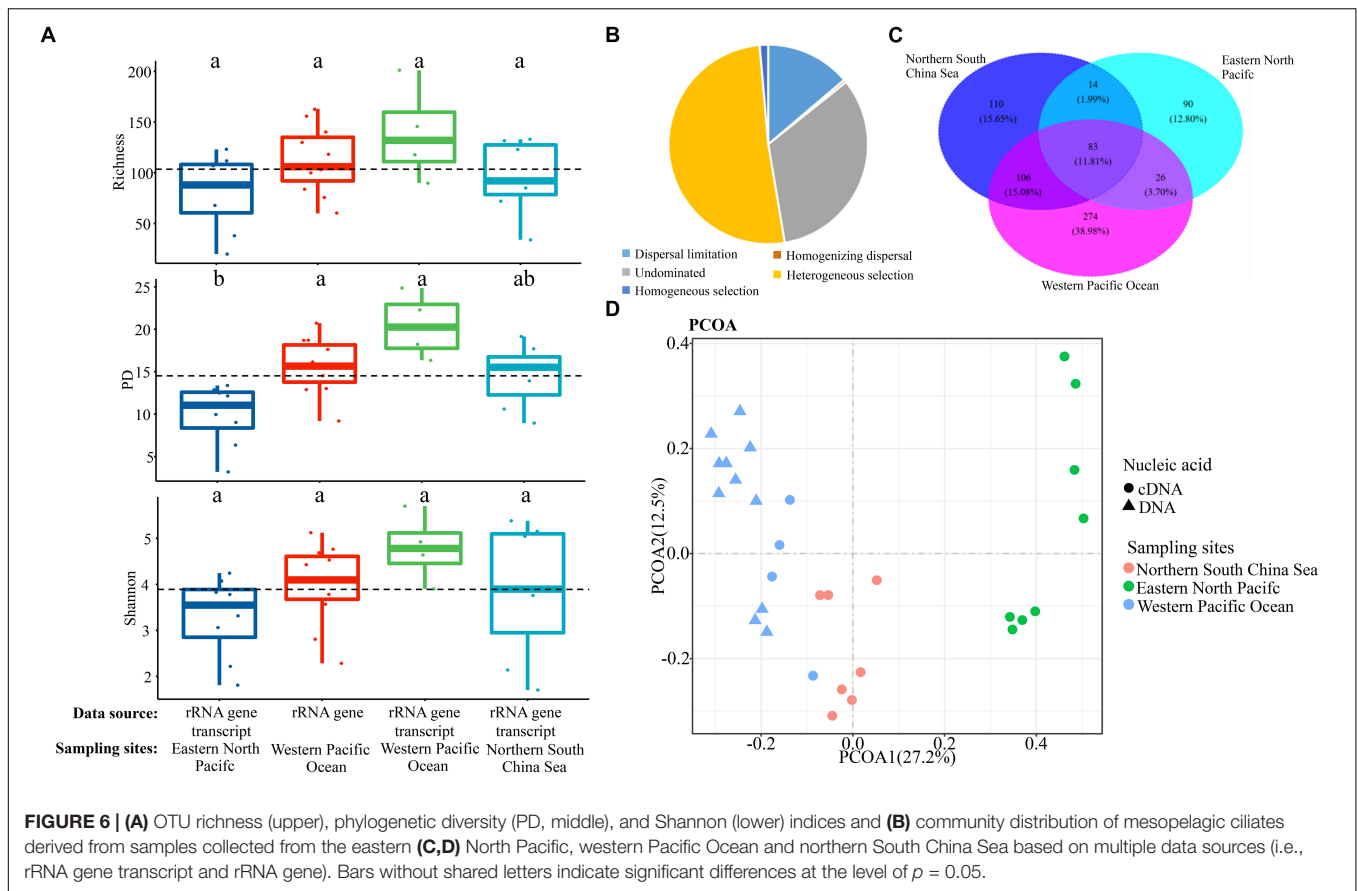


**FIGURE 5** | Alpha diversity metrics including **(A)** OTU/species richness, **(B)** Shannon's  $H'$  and **(C)** effective number of species [ $\exp(H')$ ] in vertical distribution derived from samples collected from the eastern North Pacific, western Pacific Ocean and northern South China Sea based on multiple data sources (i.e., rRNA gene transcript, rRNA gene, and morphology). To evaluate the consistency of the alpha diversity in vertical distribution among the following metrics were computed: **(A)** OTU/species richness (considering observed richness), **(B)** Shannon's  $H'$  (considering both richness and relative abundance), and **(C)** effective number of species [ $\exp(H')$ ] (considering true diversity, not indices). Bars without shared letters indicate significant differences at the level of  $p = 0.05$ .

consume bacteria in bottom waters of sampling sites (32–120 m) (Santoferrara et al., 2016). Gómez (2007) found that aloricate choreotrichs and oligotrichs were less affected than tintinnids by the reduction of food availability under oligotrophic conditions. Aloricate ciliates, therefore, would be expected to dominate the spirotrichean community in mesopelagic waters given that the food sources, e.g., pico- and nano-phytoplankton, flagellates and bacteria, are generally less accessible than in the layers above (Christaki et al., 1999; Pitta et al., 2001). Tintinnid diversity was found to more closely reflect resource

diversity than competitive interactions or predation (Dolan et al., 2002). In the present study, we found that tintinnid diversity in mesopelagic waters was much lower than that of the other layers, indicating a possible low diversity of tintinnid food source in the mesopelagic zone. Among oligohymenophoreans, the relative abundance of OTUs affiliated with Scuticociliatia increased from 65.4% in the euphotic zone to 90.7% in the mesopelagic zone. Furthermore, scuticociliates contributed 62.11% to the differences in oligohymenophorean communities down the water column. Scuticociliates are able to withstand a wide range of



salinities and are particularly abundant in habitats with high levels of organic matter, nutrients and bacteria (Urrutxurtu et al., 2003). The higher abundance of scuticociliates in mesopelagic vs. euphotic waters might be related to the reprocessing of organic matter (e.g., the sinking flux of particulates and downward advection of dissolved organic matter) as they could actively feed on particulate material and bacteria (Urrutxurtu et al., 2003; Robinson et al., 2010). In addition, some scuticociliates are opportunistic or facultative parasites and can cause severe mortalities in hosts. It has previously been reported that the diversity and abundance of parasitic ciliates in the meso- and abyssal-pelagic zones are higher than those in water layers above in the western Pacific Ocean (Weisse, 2017; Zhao et al., 2017). Similarly, molecular fragments of various parasitic protist groups were reported to contribute significant fractions of the total protist community in HTS datasets (Edgcomb, 2016). These findings suggest that parasitoid, parasitic and commensal protists, including oligohymenophoreans, are an important component of mesopelagic food chains.

The morphological dataset revealed a weak seasonal variation in ciliate communities (Table 2) whereas the molecular datasets (year 2013,  $N = 19$ ; year 2014,  $N = 22$ ; years 2013 and 2014,  $N = 41$ ) all showed an insignificant difference in community composition between spring and summer (Table 2 and Supplementary Table S6). Looking further at community variation between spring and summer in each ecological layer

using both morphological and molecular (2013 and 2014) datasets, however, revealed that significant seasonal variation only occurred at the surface layer, although the  $p$ -value of the former was much lower than that of the latter (Table 2 and Supplementary Table S6). Furthermore, neither the euphotic nor the mesopelagic layers showed significant difference in community composition between spring and summer (Table 2 and Supplementary Table S6). This suggests that the seasonal pattern of ciliate community was mainly the result of community variation in the surface layer. Variability in the surface ciliate community structure during different seasons is not surprising, and similar findings have been reported for surface communities of microbial eukaryotes in the north Pacific Ocean (Countway et al., 2010; Kim et al., 2014). Such variability is thought to be due to exposure to climatic fluctuations and the inherent patchiness of surface waters. At the USC Microbial Observatory (San Pedro Channel, North Pacific Ocean), a 10-year study by Kim et al. (2014) also found that seasonality of microeukaryote communities was not detected in deep (500 m) waters. By contrast, weekly sampling over a 6-month (January to June 2017) period at a deep-water (250 m) mesopelagic coastal site in the Mediterranean Sea revealed seasonal variation in tintinnid ciliate communities (Dolan et al., 2019). This variation was attributed to seasonal fluctuations in depth of the mixed layer which can extend to >200 m with deep water (>500 m) formation during winter (January–March) (Dolan et al., 2019). For the transect

in the present study, the mixed layer also varied with season but within a much narrower range, i.e., by approximately 11–13 m for sites C1 and C3, 20 m for sites C5 and C7, 30 m for site C9 in spring, 6 m for site C1, 7–15 m for sites C3, C5, and C7, and 20 m for site C9 in summer. Also, compared with the surface layer, horizontal advection is much weaker in the mesopelagic zone. Therefore, the insignificant temporal variation in mesopelagic ciliates might be due to temporally stable environmental conditions at this depth.

Partial Mantel test suggested that depth, geographic distance, and environmental factors played key roles in shaping ciliate community composition, with depth being the most critical (Table 3). Although a high proportion of community variation was depth-related, this might be due to depth being a proxy for various physiochemical factors in oceanic waters. For example, with increasing depth, oceanic waters are prone to become more dense with lower temperature, higher salinity, higher concentrations of dissolved organic matter and lower concentrations of oxygen, each of which is likely to influence microbial trophic function and community structure (Jiao et al., 2013; Pernice et al., 2015; Edgcomb, 2016).

Understanding the ecological processes that shape community assembly is of central importance in the field of community biology. Most previous studies, however, have focused on either prokaryotes (Burke et al., 2011) or plants and animals (Kraft and Ackerly, 2014). The processes that shape community assembly of microeukaryotes in general (Logares et al., 2018), and ciliates in particular (Dolan et al., 2007), remain poorly understood. The employment of phylogenetic null model analysis makes determination and quantification of ecological processes possible (Stegen et al., 2013). This approach has limitations, e.g., the framework is unable to differentiate biological interaction, such as competition and trophic interactions, from selection and is subjective to methodological artifacts such as PCR-bias and DNA sequencing errors (Stegen et al., 2013). Nevertheless, it has been accepted as an effective means of analyzing community assembly of microbes in a variety of environments (Bahram et al., 2015; Dini-Andreote et al., 2015; Logares et al., 2018). This study is the first to use this framework to address the assembly mechanisms of ciliate communities. Dispersal limitation was found to be the most important ecological process shaping ciliate communities, followed by heterogeneous selection and ecological drift (Figure 3). The many physical and biogeochemical features of water across depth strata represent a highly heterogeneous set of environments that generates different vertical ecological layers and a strong response by the ciliate community to environmental selection and dispersal limitation. In surface waters, heterogeneous selection contributed a much higher proportion of the community variation than did dispersal limitation (Figure 3). This contrasts with the situation in the euphotic and mesopelagic zones, indicating that assembly mechanisms in surface waters differs from those deeper in the water column. Unlike the euphotic and mesopelagic zones, the surface is generally characterized by higher fluctuations of salinity and temperature and stronger mixing by wind leading to higher environmental filtering and lower dispersal limitations (Wu et al., 2017). On the other hand, wind-induced mixing would generate

a relatively homogeneous environment (Wu et al., 2017). This is likely the reason why homogeneous dispersal was observed only in surface waters, albeit with a relatively small contribution (Figure 3). Compared with the surface layer, horizontal mixing is much weaker in deeper waters, therefore the impact of dispersal limitation is greater in the euphotic and mesopelagic zones. The transitional layer between the base of euphotic zone and the top of mesopelagic zone showed that environmental selection was primarily responsible for determining ciliate community structure. This layer represents a depth of major transitions of several environmental factors. Therefore, a stronger response of the ciliate community to selection was found in transitional layer than in other water layers.

## Mesopelagic Ciliates Across Oceanic Basins

Only a limited number of studies on spatio-temporal distributions of ciliates down the water column have been performed, especially in the mesopelagic zone (Wickham et al., 2011; Hu et al., 2016). Therefore, it is difficult to carry out regional comparisons of vertical distribution of mesopelagic ciliate diversity. By downloading 18S rRNA V4 region sequences derived from two pilot studies carried out in the western Pacific Ocean (Zhao et al., 2017) and eastern North Pacific (Hu et al., 2016) and analyzing these along with the present data from the SCS, we found that ciliate diversity in the mesopelagic zone was comparable to that of surface water in each of the three ocean basins regardless of the type of dataset analyzed, i.e., rRNA gene, rRNA gene transcript or morphology (Figure 5). This suggests that the high ciliate diversity in the mesopelagic zone is a general phenomenon. Mesopelagic communities showed a large variability across oceanic basins, as seen by the distribution of samples in the PCoA (Figure 6D) and statistical results of ANOSIM (Supplementary Table S9). Mesopelagic ciliate communities showed a clear distance-decay pattern (Supplementary Figure S7) in that the similarity of community composition decreased with geographic distance increased. This phenomenon could explain why community similarity between the two geographically close basins, i.e., northern SCS and western Pacific Ocean, was higher than those of other pairwise comparisons, i.e., northern SCS and eastern North Pacific Ocean, western Pacific and eastern North Pacific Oceans (Figure 6D and Supplementary Table S9). Similar results were reported for microeukaryotes in abyssal waters across world's oceans, the similarity of environmental conditions shaping the microbial communities in nearby sites being cited as the most plausible cause (Pernice et al., 2015). Using the null modeling approach, it was found that heterogeneous selection was the primary factor determining mesopelagic ciliate community assembly across oceanic basins (Figure 6B). Therefore, the large proportion of unique OTUs of each basin (Figure 6C), and distinct community composition across basins (Figure 6D and Supplementary Table S9), could be mainly the result of environmental selection. This is consistent with the findings for microeukaryotes in surface (Massana and Logares, 2013) and deep waters (Pernice et al., 2015). It should be noted, however,

that the distribution pattern seen in **Figure 6D** could also be an artifact that reflects the differences in procedures for dealing with samples between the present and the previous studies (Hu et al., 2016; Zhao et al., 2017). Study-specific factors, e.g., amount of water sampled for nucleic acid extraction, extraction and PCR protocols, and sequencing depth, could strongly influence the results. Therefore, standard operating procedures of sampling and data processing should be established and taken into consideration in future studies. Collectively, these findings suggest that mesopelagic ciliates across oceanic basins exhibit high diversity, and their biogeography could be mainly shaped by environmental selection. Future studies on a wider range of protist groups over broader temporal scales and across other ocean basins, water masses or biogeochemical provinces are needed to determine whether this pattern of diversity is widely applicable.

## Community Composition Revealed by Molecular- and Morphology-Based Methods

Previous studies indicated that HTS can detect species present in low abundance in a sample and therefore holds the potential to retrieve components of diversity not evident using traditional morphological methods (Sogin et al., 2006). In the present study, HTS revealed more diverse assemblages of ciliates than microscopic examination of specimens prepared by QPS leading to the result that the community composition disclosed by the two approaches did not match perfectly. For example, Colpodea and Phyllopharyngea contributed ca. 13.1 and 23.5% of the ciliate community in molecular datasets, respectively, but were undetected by QPS (**Supplementary Figure S8a**). This might be due to the differences inherent to the molecular/morphology-based methods, e.g., cell loss during sample processing and preservation (Pfister et al., 1999; Sonntag et al., 2000). Also, variation in rDNA copy number among different lineages of ciliates could confuse the comparison between morphological and molecular methods (Wang et al., 2017). In the present study, rRNA-based amplification was applied in order to mitigate the impact of this, nevertheless variations in copy number can still influence community composition based on rRNA datasets. Similarly, in a survey on ciliates from the surface to the abyssopelagic zone in the Western Pacific Ocean, Zhao et al. (2017) found Phyllopharyngea to be much more diverse and abundant in the community derived from cDNA than DNA sequencing. In addition, activity, growth rate, cell size and biomass could also contribute to varying amounts of rRNA in ciliates (Fu and Gong, 2017) and thus strongly influence the community composition revealed by the two approaches.

Overall, both methods showed the major contributors of ciliate community at class level, indicating community composition at high taxonomic level revealed by HTS and QPS are comparable (**Supplementary Figure S8a**). Congruence generally decreased, however, when moving down the taxonomic hierarchy from class to genus (**Supplementary Figures S8a–d**). Among 79 morphospecies, 78 were assignable to class, 64 to order, 64 to family and 59 to genus. For the molecular

dataset, 571 of 575 OTUs were assignable to class, 368 to order, 349 to family and 227 to genus. Therefore, it is difficult to compare the differences in community composition at lower taxonomic levels revealed by the two approaches. For instance, if an OTU is lacking an affiliation to an order, then it is impossible to determine its identity at any rank below class. In the present study, approximately 19% of morphospecies and 36% of OTUs could not be assigned to any known order. Comparison of composition at lower taxonomic levels as revealed by the two approaches therefore becomes inappropriate and inaccurate under these circumstances. This also corresponds with the findings of previous studies where both methods have been applied, i.e., on tintinnid ciliates from coastal waters (Bachy et al., 2013; Santoferrara et al., 2014) or planktonic ciliates from mountain lakes (Stoeck et al., 2014; Pitsch et al., 2019), which have also reported a gap between molecular and morphological methods for revealing community composition at lower taxonomic ranks.

Unassigned/unidentified taxa generally occupy higher proportions in molecular datasets than in morphological datasets, suggesting that the reference databases for assigning environmental sequences to different taxonomic ranks remain far from being sufficiently well-represented. In this study, Oligotrichia and Choreotrichia were the top two abundant assemblages in the morphological dataset, accounting for 31.33 and 28.35% of total species abundance, respectively. For species of Oligotrichia, only four out of 22 species have a V4 18S rRNA sequence in the PR2 database (version 4.7.2). Likewise, none of the nine aloricate choreotrichians and only seven out of 19 loricate choreotrichians could be related to a named sequence in the database. The lack of sufficient sequence information for a given morphospecies might also contribute to the discrepancy between morphological and molecular datasets. Furthermore, errors in the reference database could also confuse the interpretation, such as: (i) taxonomic classification is not always consistent at each rank, e.g., name of subclass occurred at the place where order name should be given; (ii) the classification used is inconsistent as taxonomic and molecular classifications are sometimes incongruent; (iii) sequences annotated with a species name sometimes have ambiguous names at higher taxonomic ranks; (iv) multiple sequences may bear the same species name, e.g., 15 different sequences are registered in the database under the species name *Peritromus kahli*. Therefore, the discrepancy between ciliate community composition revealed by HTS and QPS seen in this study is consistent with previous findings for other assemblages of microbial eukaryotes (Egge et al., 2013). This suggests that direct comparisons in community composition revealed by the two methods at low taxonomic ranks are not applicable.

Despite the inherent limitation of the comparison between morphological and molecular methods, the distribution patterns of the ciliate communities disclosed by the two methods generally agree with each other (**Figure 1C**, **Supplementary Figure S3c**, **Table 2**, and **Supplementary Table S6**). Both approaches revealed a vertical distribution pattern, and a seasonal variation for surface ciliate communities, confirming the existence of a spatiotemporal distribution pattern the studied area. Similar findings were also

reported for tintinnid ciliates across a coast-to-ocean transect off the coast of Rhode Island (United States) (Santoferrara et al., 2016). Employing morphological and molecular approaches, there was general agreement in the distribution patterns recovered and in the correlations with environmental parameters (Santoferrara et al., 2016). In the present study, however, the molecular method showed a nearshore-offshore distribution whereas this was not recovered by the morphological method (Table 2 and Supplementary Table S6). This could be due to the differences inherent in the two approaches discussed earlier. For example, members of abundant and rare species can be detected by HTS but this is subject to variation of rRNA gene copy number between individuals/species (Wang et al., 2017). QPS is exempt from the issue of rRNA gene copy numbers but has low power in detecting rare species (Bachy et al., 2013; Santoferrara et al., 2016). Therefore, it is recommended that an integrated approach, combining morphological and molecular methods, should be employed to study the diversity and distribution of ciliates in order to mitigate the limitations of using one method alone.

In summary, mesopelagic ciliates exhibited comparable alpha diversity to that of surface communities in the northern SCS and this distribution pattern was consistent temporally and across two other oceanic basins. Mesopelagic ciliates harbored distinct community structure with insignificant differences occurring temporally. Additionally, dispersal limitation was found to override heterogeneous selection in determining mesopelagic ciliate community assembly. Due to the number of mesopelagic samples collected being limited to two sites, the aim of identifying the spatially dynamic pattern of mesopelagic ciliates in the SCS could not be met. In future studies, spatial sampling on a wider scale should be conducted to confirm the patterns observed here. An integrative approach combining multiple sources of information, e.g., morphology, molecular and ecology, is needed in order to characterize the community dynamics of mesopelagic ciliates.

## REFERENCES

- Bachy, C., Dolan, J. R., Deschamps, P., and Moreira, D. (2013). Accuracy of protist diversity assessments: morphology compared with cloning and direct pyrosequencing of 18S rRNA genes and ITS regions using the conspicuous tintinnid ciliates as a case study. *ISME J.* 7, 244–255. doi: 10.1038/ismej.2012.106
- Bahram, M., Peay, K. G., and Tedersoo, L. (2015). Local-scale biogeography and spatiotemporal variability in communities of mycorrhizal fungi. *New Phytol.* 205, 1454–1463. doi: 10.1111/nph.13206
- Bolger, A. M., Lohse, M., and Usadel, B. (2014). Trimmomatic: a flexible trimmer for Illumina sequence data. *Bioinformatics* 30, 2114–2120. doi: 10.1093/bioinformatics/btu170
- Burke, C., Steinberg, P., Rusch, D., Kjelleberg, S., and Thomas, T. (2011). Bacterial community assembly based on functional genes rather than species. *Proc. Natl. Acad. Sci. U.S.A.* 108, 14288–14293. doi: 10.1073/pnas.1101591108
- Chao, A., and Shen, T. J. (2003). *Program SPADE (Species Prediction and Diversity Estimation). Program and User's Guide.* Available at <http://chao.stat.nthu.edu.tw> (accessed May, 2019).
- Chase, J. M., Kraft, N. J. B., Smith, K. G., Vellend, M., and Inouye, B. D. (2011). Using null models to disentangle variation in community dissimilarity from variation in  $\alpha$ -diversity. *Ecosphere* 2, 1–11.
- Christaki, U., Wambeke, F. V., and Dolan, J. R. (1999). Nanoflagellates (mixotrophs, heterotrophs and autotrophs) in the oligotrophic eastern

## DATA AVAILABILITY STATEMENT

The datasets generated for this study can be found in the NCBI Sequence Read Archive (Accession Code SRP182690).

## AUTHOR CONTRIBUTIONS

PS conceived and designed the study. LH conducted the experiments. LW, WX, and JK collected the samples. PS, LH, and YW analyzed the data. All authors wrote the manuscript.

## FUNDING

BH and PS appreciate the National Key Research and Development Program of China (No. 2016YFA0601202). PS also thanks to NSFC (31772426 and U1805241) and Natural Science Foundation of Fujian Province (2017J01080). DX acknowledges NSFC (41876142).

## ACKNOWLEDGMENTS

We are grateful to Dr. Jianyu Hu for kindly providing CTD data and to Dr. Fan Zhang for the nutrients data. We thank the crew of R/V Yanping II for facilitating field sampling.

## SUPPLEMENTARY MATERIAL

The Supplementary Material for this article can be found online at: <https://www.frontiersin.org/articles/10.3389/fmicb.2019.02178/full#supplementary-material>

- Mediterranean: standing stocks, bacterivory and relationships with bacterial production. *Mar. Ecol. Prog. Ser.* 181, 297–307. doi: 10.3354/meps181297
- Clarke, K. R., and Gorley, R. N. (2009). *PRIMER v6: User Manual/Tutorial.* Plymouth: PRIMER-E.
- Countway, P. D., Vigil, P. D., Schnetzer, A., Moorthi, S. D., and Caron, D. A. (2010). Seasonal analysis of protistan community structure and diversity at the USC microbial observatory (San Pedro Channel, North Pacific Ocean). *Limnol. Oceanogr.* 55, 44–51. doi: 10.4319/lo.2010.55.6.2381
- Dehairs, F., Shopova, D., Ober, S., Veth, C., and Goeyens, L. (1997). Particulate barium stocks and oxygen consumption in the Southern Ocean mesopelagic water column during spring and early summer: relationship with export production. *Deep Sea Res. Part II Topical Stud. Oceanogr.* 44, 497–516. doi: 10.1016/S0967-0645(96)00072-0
- Dini-Andreote, F., Stegen, J. C., van Elsas, J. D., and Salles, J. F. (2015). Disentangling mechanisms that mediate the balance between stochastic and deterministic processes in microbial succession. *Proc. Natl. Acad. Sci. U.S.A.* 112, E1326–E1332. doi: 10.1073/pnas.1414261112
- Doherty, M., Tamura, M., Costas, B. A., Ritchie, M. E., McManus, G. B., and Katz, L. A. (2010). Ciliate diversity and distribution across an environmental and depth gradient in long Island sound, USA. *Environ. Microbiol.* 12, 886–898. doi: 10.1111/j.1462-2920.2009.02133.x
- Dolan, J., Ritchie, M., and Ras, J. (2007). The "neutral" community structure of planktonic herbivores, tintinnid ciliates of the microzooplankton, across the SE



- tropical pacific ocean. *Biogeosci. Discuss.* 4, 561–593. doi: 10.5194/bg-4-297-2007
- Dolan, J. R., Ciobanu, M., Marro, S., and Coppola, L. (2019). An exploratory study of heterotrophic protists of the mesopelagic Mediterranean Sea. *ICES J. Mar. Sci.* 76, 616–625. doi: 10.1093/icesjms/fix218
- Dolan, J. R., Claustre, H., Carlotti, F., Plounevez, S., and Moutin, T. (2002). Microzooplankton diversity: relationships of tintinnid ciliates with resources, competitors and predators from the atlantic coast of morocco to the eastern mediterranean. *Deep Sea Res. Part I Oceanogr. Res. Pap.* 49, 1217–1232. doi: 10.1016/s0967-0637(02)00021-3
- Dopheide, A., Lear, G., Stott, R., and Lewis, G. (2008). Molecular characterization of ciliate diversity in stream biofilms. *Appl. Environ. Microbiol.* 74, 1740–1747. doi: 10.1128/AEM.01438-07
- Dufrene, M., and Legendre, P. (1997). Species assemblages and indicator species: the need for a flexible asymmetrical approach. *Ecol. Monogr.* 67, 345–366. doi: 10.1890/0012-9615
- Edgar, R. C. (2010). Search and clustering orders of magnitude faster than BLAST. *Bioinformatics* 26, 2460–2461. doi: 10.1093/bioinformatics/btq461
- Edgar, R. C., Haas, B. J., Clemente, J. C., Quince, C., and Knight, R. (2011). UCHIME improves sensitivity and speed of chimera detection. *Bioinformatics* 27, 2194–2200. doi: 10.1093/bioinformatics/btr381
- Edgcomb, V. P. (2016). Marine protist associations and environmental impacts across trophic levels in the twilight zone and below. *Curr. Opin. Microbiol.* 31, 169–175. doi: 10.1016/j.mib.2016.04.001
- EGGE, E., Bittner, L., Andersen, T., Audic, S., Vargas, C. D., and Edvardsen, B. (2013). 454 Pyrosequencing to describe microbial eukaryotic community composition, diversity and relative abundance: a test for marine haptophytes. *PLoS One* 8:e74371. doi: 10.1371/journal.pone.0074371
- Fu, R., and Gong, J. (2017). Single cell analysis linking ribosomal (r)DNA and rRNA copy numbers to cell size and growth rate provides insights into molecular protistan ecology. *J. Eukaryot. Microbiol.* 64, 885–896. doi: 10.1111/jeu.12425
- Gómez, F. (2007). Trends on the distribution of ciliates in the open pacific ocean. *Acta Oecol.* 32, 188–202. doi: 10.1016/j.actao.2007.04.002
- Gowing, M. M., Garrison, D. L., Wishner, K. F., and Gelfman, C. (2003). Mesopelagic microplankton of the Arabian Sea. *Deep Sea Res. Part I* 50, 1205–1234. doi: 10.1016/S0967-0637(03)00130-4
- Grattepanche, J. D., Santoferrara, L. F., Mcmanus, G. B., and Katz, L. A. (2016). Unexpected biodiversity of ciliates in marine samples from below the photic zone. *Mol. Ecol.* 25, 3987–4000. doi: 10.1111/mec.13745
- Guillou, L., Bachar, D., Audic, S., Bass, D., Bernery, C., Bittner, L., et al. (2013). The protist ribosomal reference database (PR2): a catalog of unicellular eukaryote small sub-unit rRNA sequences with curated taxonomy. *Nucleic Acids Res.* 41, 597–604. doi: 10.1093/nar/gks1160
- Hu, J., Liu, X., Zhang, F., Huang, B. Q., and Hong, H. S. (2008). Study on nutrient limitation of phytoplankton in southern Taiwan Strait during the summer. *J. Oceanogr. Taiwan Strait.* 27, 452–458. doi: 10.3724/SP.J.1035.2008.00038
- Hu, J. Y., Hong, H. S., Li, Y., Jiang, Y., Chen, Z., Zhu, J., et al. (2011). Variable temperature, salinity and water mass structures in the southwestern taiwan strait in summer. *Con. Shelf Res.* 31, S13–S23. doi: 10.1016/j.csr.2011.02.003
- Hu, S. K., Campbell, V., Connell, P., Gellene, A. G., Liu, Z., Terrado, R., et al. (2016). Protistan diversity and activity inferred from RNA and DNA at a coastal ocean site in the eastern North Pacific. *FEMS Microbiol. Ecol.* 92:fiw050. doi: 10.1093/femsec/fiw050
- Huang, B. Q., Hu, J., Xu, H. Z., Cao, Z. R., and Wang, D. X. (2010). Phytoplankton community at warm eddies in the northern South China Sea in winter 2003/2004. *Deep Sea Res. Part II* 57, 1792–1798. doi: 10.1016/j.dsr2.2010.04.005
- Jiao, N., Luo, T., Zhang, R., Yan, W., Lin, Y., Johnson, Z. L., et al. (2013). Presence of *Prochlorococcus* in the aphotic waters of the western Pacific Ocean. *Biogeosciences* 10, 9345–9371. doi: 10.5194/bg-11-2391-2014
- Kim, D. Y., Countway, P. D., Jones, A. C., Schnetzer, A., Yamashita, W., Tung, C., et al. (2014). Monthly to interannual variability of microbial eukaryote assemblages at four depths in the eastern North Pacific. *ISME J.* 8, 515–530. doi: 10.1038/ismej.2013.173
- Kofoid, C. A., and Campbell, A. S. (1929). A conspectus of the marine and freshwater Ciliata belonging to the suborder Tintinnoinea, with descriptions of new species, principally from the agassiz expedition to the eastern tropical pacific, 1904–1905. *Univ. Calif. Publ. Zool.* 34, 1–403.
- Kofoid, C. A., and Campbell, A. S. (1939). The ciliata: the tintinnoinea. reports on the scientific results of the expedition to the eastern tropical pacific, 1904–1905. *Bull. Mus. Comp. Zool. Harv.* 84, 1–473.
- Kraft, N. J. B., and Ackerly, D. D. (2014). “Assembly of plant communities,” in *Ecology and the Environment*, ed. R. K. Monson (New York, NY: Springer).
- Legendre, P., and Legendre, L. (1998). *Numerical ecology*. Netherlands: Elsevier.
- Liang, W. D., Yang, Y. J., Tang, T. Y., and Chuang, W. S. (2008). Kuroshio in the Luzon Strait. *J. Geophys. Res.* 113, C08048. doi: 10.1029/2007JC004609
- Logares, R., Tesson, S., Canbäck, B., Pontarp, M., Hedlund, K., and Rengefors, K. (2018). Contrasting prevalence of selection and drift in the community structuring of bacteria and microbial eukaryotes. *Environ. Microbiol.* 20, 1–15. doi: 10.1111/1462-2920.14265
- Lynn, D. H., Montagnes, D. J. S., and Small, E. B. (1988). Taxonomic descriptions of some conspicuous species in the family Strombidiidae (Ciliophora: Oligotrichida) from the Isles of Shoals, Gulf of Maine. *J. Mar. Biol. Assoc. U.K.* 68, 259–276. doi: 10.1017/S0025315400052176
- Magoč, T., and Salzberg, S. L. (2011). FLASH: fast length adjustment of short reads to improve genome assemblies. *Bioinformatics* 27, 2957–2963. doi: 10.1093/bioinformatics/btr507
- Massana, R., and Logares, R. (2013). Eukaryotic versus prokaryotic marine picoplankton ecology. *Environ. Microbiol.* 15, 1254–1261. doi: 10.1111/1462-2920.12043
- Montagnes, D., and Lynn, D. (1993). A quantitative protargol stain (QPS) for ciliates and other protists. *Handb. Methods Aquat. Microb. Ecol.* 27, 229–240. doi: 10.1201/9780203752746-28
- Morton, B., and Blackmore, G. (2001). South China Sea. *Mar. Poll. Bull.* 42, 1236–1263. doi: 10.1016/S0025-326X(01)00240-5
- Pernice, M. C., Giner, C. R., Logares, R., Pererabel, J., Acinas, S. G., Duarte, C. M., et al. (2015). Large variability of bathypelagic microbial eukaryotic communities across the world's oceans. *ISME J.* 10, 945–958. doi: 10.1038/ismej.2015.170
- Pfister, G., Sonntag, B., and Posch, T. (1999). Comparison of a direct live count and an improved quantitative protargol stain (QPS) in determining abundance and cell volumes of pelagic freshwater protozoa. *Aquat. Microb. Ecol.* 18, 95–103. doi: 10.3354/ame018095
- Pitsch, G., Bruni, E. P., Forster, D., Qu, Z., Sonntag, B., Stoeck, T., et al. (2019). Seasonality of planktonic freshwater ciliates: are analyses based on v9 regions of the 18S rRNA gene correlated with morphospecies counts? *Front. Microbiol.* 10:248. doi: 10.3389/fmicb.2019.00248
- Pitta, P., Giannakourou, A., and Christaki, U. (2001). Planktonic ciliates in the oligotrophic mediterranean Sea: longitudinal trends of standing stocks, distributions and analysis of food vacuole contents. *Aquat. Microb. Ecol.* 24, 297–311. doi: 10.3354/ame024297
- Robinson, C., Steinberg, D. K., Anderson, T. R., Aristegui, J., Carlson, C. A., Frost, J. R., et al. (2010). Mesopelagic zone ecology and biogeochemistry—a synthesis. *Deep Sea Res. Part II Topical Stud. in Oceanogr.* 57, 1504–1518. doi: 10.1016/j.dsr2.2010.02.018
- Santoferrara, L. F., Grattepanche, J. D., Katz, L. A., and Mcmanus, G. B. (2014). Pyrosequencing for assessing diversity of eukaryotic microbes: analysis of data on marine planktonic ciliates and comparison with traditional methods. *Environ. Microbiol.* 16, 2752–2763. doi: 10.1111/1462-2920.12380
- Santoferrara, L. F., Grattepanche, J. D., Katz, L. A., and Mcmanus, G. B. (2016). Patterns and processes in microbial biogeography: do molecules and morphologies give the same answers? *ISME J.* 10, 1779–1790. doi: 10.1038/ismej.2015.224
- Sogin, M. L., Morrison, H. G., Huber, J. A., Mark, W. D., Huse, S. M., Neal, P. R., et al. (2006). Microbial diversity in the deep sea and the underexplored “rare biosphere”. *Proc. Natl. Acad. Sci. U.S.A.* 103, 12115–12120. doi: 10.1073/pnas.0605127103
- Song, W., Warren, A., and Hu, X. (2009). *Free-Living Ciliates in the Bohai and Yellow Seas*. China: Science. Press.
- Sonntag, B., Psenner, R., and Posch, T. (2000). Comparison of three methods for determining flagellate abundance, cell size, and biovolume in cultures and natural freshwater samples. *Arch. Hydrobiol.* 149, 337–351. doi: 10.1016/S0166-445X(00)00105-3
- Stegen, J. C., Lin, X., Fredrickson, J. K., Chen, X., Kennedy, D. W., Murray, C. J., et al. (2013). Quantifying community assembly processes and identifying features that impose them. *ISME J.* 7, 2069–2079. doi: 10.1038/ismej.2013.93

- Stoeck, T., Bass, D., Nebel, M., Christen, R., Jones, M. D. M., Breiner, H. W., et al. (2010). Multiple marker parallel tag environmental DNA sequencing reveals a highly complex eukaryotic community in marine anoxic water. *Microb. Ecol.* 19, 21–31. doi: 10.1111/j.1365-294X.2009.04480.x
- Stoeck, T., Breiner, H. W., Filker, S., Ostermaier, V., Kammerlander, B., and Sonntag, B. (2014). A morphogenetic survey on ciliate plankton from a mountain lake pinpoints the necessity of lineage-specific barcode markers in microbial ecology. *Environ. Microbiol.* 16, 430–444. doi: 10.1111/1462-2920.12194
- Tanaka, T., and Rassoulzadegan, F. (2002). Full-depth profile (0–2000 m) of bacteria, heterotrophic nanoflagellates and ciliates in the NW mediterranean Sea: vertical partitioning of microbial trophic structures. *Deep Sea Res. II* 49, 2093–2107. doi: 10.1016/S0967-0645(02)00029-2
- Urrutxurtu, E., Orive, E., and Sota, A. D. L. (2003). Seasonal dynamics of ciliated protozoa and their potential food in an eutrophic estuary (bay of Biscay). *Estuar. Coast. Shelf S.* 57, 1169–1182. doi: 10.1016/S0272-7714(03)00057-X
- Wang, C., Zhang, T., Wang, Y., Katz, L. A., Gao, F., and Song, W. (2017). Disentangling sources of variation in SSU rDNA sequences from single cell analyses of ciliates: impact of copy number variation and experimental error. *Proc. R. Soc. B* 284:20170425. doi: 10.1098/rspb.2017.0425
- Weisse, T. (2017). Functional diversity of aquatic ciliates. *Eur. J. Protistol.* 61, 331–358. doi: 10.1016/j.ejop.2017.04.001
- Wickham, S. A., Steinmair, U., and Kamennaya, N. A. (2011). Ciliate distributions and forcing factors in the Amundsen and Bellingshausen Seas (Antarctic). *Aquat. Microb. Ecol.* 62, 215–230. doi: 10.3354/ame01468
- Wu, W. X., Logares, R., Huang, B. Q., Wu, W., and Hsieh, C. H. (2017). Abundant and rare picoeukaryotic sub-communities present contrasting patterns in the epipelagic waters of marginal seas in the northwestern pacific ocean. *Environ. Microbiol.* 19, 287–300. doi: 10.1111/1462-2920.13606
- Zhao, F., Filker, S., Xu, K., Huang, P., and Zheng, S. (2017). Patterns and drivers of vertical distribution of the ciliate community from the surface to the abyssopelagic zone in the western pacific ocean. *Front. Microbiol.* 8:2559. doi:10.3389/fmicb.2017.02559
- Zhou, J., and Ning, D. (2017). Stochastic community assembly: does it matter in microbial ecology? *Microbiol. Mol. Biol. Rev.* 81:e00002–17. doi: 10.1128/MMBR.00002-17
- Conflict of Interest:** The authors declare that the research was conducted in the absence of any commercial or financial relationships that could be construed as a potential conflict of interest.
- Copyright © 2019 Sun, Huang, Xu, Warren, Huang, Wang, Wang, Xiao and Kong. This is an open-access article distributed under the terms of the Creative Commons Attribution License (CC BY). The use, distribution or reproduction in other forums is permitted, provided the original author(s) and the copyright owner(s) are credited and that the original publication in this journal is cited, in accordance with accepted academic practice. No use, distribution or reproduction is permitted which does not comply with these terms.